Master's Thesis

Investigation of NASICON Ceramics Stability Against Seawater at Room Temperature

Muhammad Fahmi Rahman

Department of Energy Engineering

(Battery Science and Technology)

Graduate School of UNIST

2019

Investigation of NASICON Ceramics Stability Against Seawater at Room Temperature

Muhammad Fahmi Rahman

Department of Energy Engineering
(Battery Science and Technology)

Graduate School of UNIST

Investigation of NASICON Ceramics Stability Against Seawater at Room Temperature

A thesis/dissertation
submitted to the Graduate School of UNIST
in partial fulfillment of the
requirements for the degree of
Master of Science

Muhammad Fahmi Rahman

01/08/2019

Approved by

Advisor
Youngsik Kim

Investigation of NASICON Ceramics Stability Against Seawater at Room Temperature

Muhammad Fahmi Rahman

This certifies that the thesis/dissertation of M. Fahmi Rahman is approved.

01/08/2019

signature

Advisor: Youngsik Kim

signature

Yunseok Choi: Thesis Committee Member #1

signature

Hyun-Wook Lee: Thesis Committee Member #2

Abstract

The trend of renewable energy has been growing around the world and an energy storage system is used to compliment the disadvantage that comes from the unreliability of renewable energy. A novel energy storage system (ESS) by harnessing the Sodium-ions from natural ions exist in seawater has been proposed and named as seawater battery. The component of seawater battery almost similar as a conventional battery, but with the addition solid electrolyte component. Solid electrolyte plays a major role in seawater battery system by the physically separate anode and cathode while maintaining Sodium-ions transportation, and Na-Superionic conductor (NASICON, $Na_3Zr_2Si_2PO_{12}$) is the most suitable candidate among all other material. However, the application of NASICON in the seawater battery system for a long-term period is questionable since NASICON was known to be unstable with water at the extreme condition. On the other hand, the stability in room temperature water and seawater is not widely research. Thus, this thesis purpose is to confirm the stability in seawater by comparison with D.I. water immersion.

To test the stability at room temperature, NASICON is immersed in D.I. water and seawater at room temperature for a long period of time (≈ 365 days) and immersed NASICON and solution are analyzed. Based on the analysis, this report found three different reactions when NASICON in contact with water and seawater, which are secondary phase dissolution, Sodium-ions diffusion, and Hydronium-ions insertion. The first two reactions slightly change the properties of NASICON while the Hydronium-ions insertion decreases the conductivity dramatically and may break NASICON with further substitution. This reaction is affected by three variables such as pH of the solution, temperature, and ions existed in the solution. Thanks to the natural-ions contained inside the seawater, the NASICON doesn’t show any sign of Hydronium-ions insertion even after 365 days immersion.

Contents

List of figures

Figure 43. a) XRD result of NASICON immersion in D.I. water, 0.1 M NaCl at 80^{o}C, and Seawater for 30 days, b) pellet after 30 days immersion at 80^{o}C, and the reference intensity ratio (RIR) at peak 29.7^{o} of NASICON immersed at the different salt solutions (concentration based on the seawater) at 80^{o}C

Figure 44. a) Ionic conductivity NASICON immersed in D.I. water and seawater after a certain time (up to 180 days) and b) EIS result after 90 days immersion

Figure 45. a) The XRD and b) EIS result of 90-day immersed NASICON before and after polished

Figure 46. Illustration of Sodium diffusion and Hydronium-ions insertions in NASICON immersion at any solution

List of table

1. Introduction

1.1. Future of renewable energy

Non-renewable energy is currently dominating the energy consumption for electricity and Non-renewable energy produced 70% of world electricity generation out of approximate 22,000 TW h (Figure 1a). [1][2] Although non-renewable energy is favorable economically, however, non-renewable energy produced greenhouse gasses such as CO_2, and around 70% of these gasses come from the energy sectors (Figure 1b). [3][4] With the rise of CO_2 emission every year (Figure 1c), the excess greenhouse gasses may bring significant effect to the world temperature, which affects not only environment but also species. [4][5] To combat this problem, the non-renewable energy needs to be reduced and replaced by renewable energy. [3]

The development in renewable energy has greatly researched since the oil crisis in 1973, but the renewable energy wasn't popular until the 1990s. In the case of wind energy, the growth was rapid in 1980-1998, which was approximately 55% annually (Figure 2a), while solar energy increased roughly 22% in the 1990s (Figure 2b). [6] The problem with renewable energy resources is they are often dependence with the environment, therefore renewable energy is geographically restricted and unreliable. For example, solar energy can't generate power at night and the power is reduced during cloudy days (Figure 4a). On the other hand, the wind energy changed over time and the maximum output generated at night (Figure 4b). With the human energy consumption that always constant, renewable energy needs to be constant and reliable anytime. Thus, the energy storage system (ESS) is introduced to solve this issue by storing energy at off-peak times and discharge during peak times. [7]

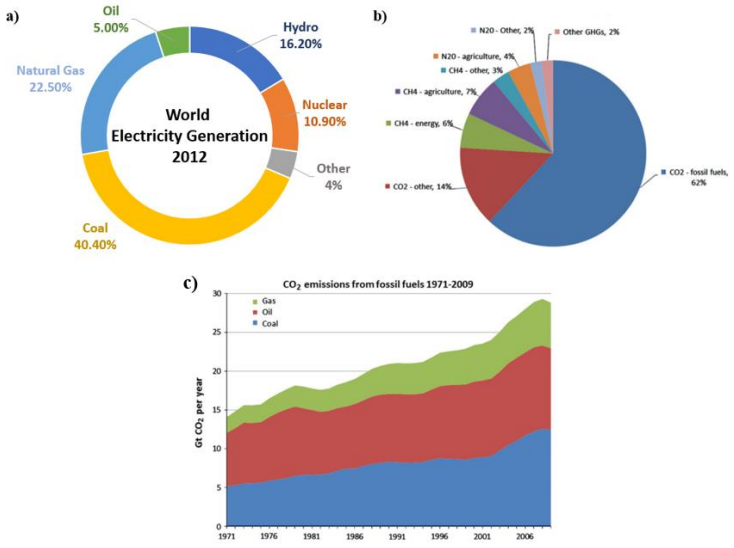

Figure 1. a) World electricity generation, b) Global greenhouse gases emission at 2008, and c) CO2 emissions from fossil fuels from 1971-2009. [2][4]

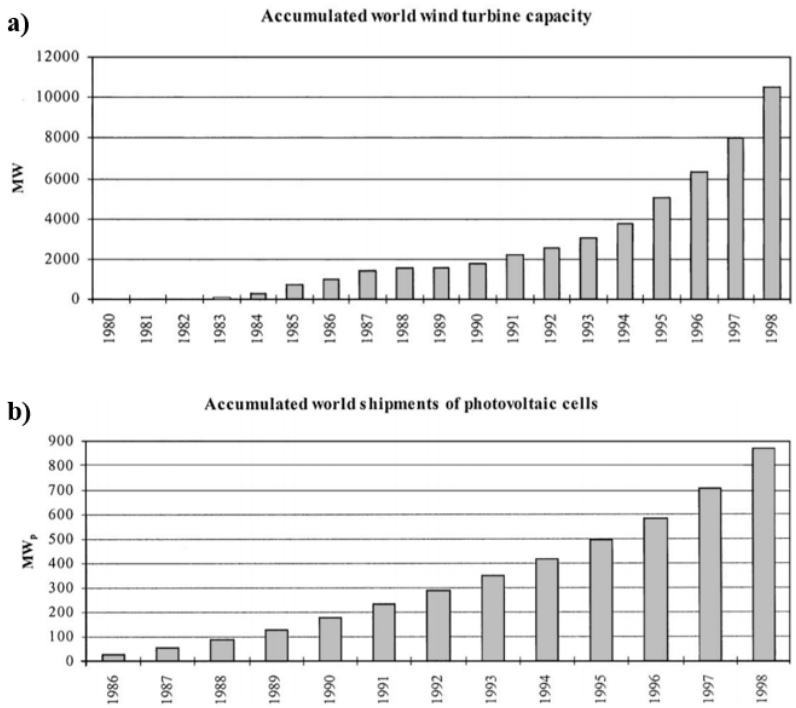

Figure 2. Accumulated a) world wind turbine capacity and b) world shipment of photovoltaic cells [6]

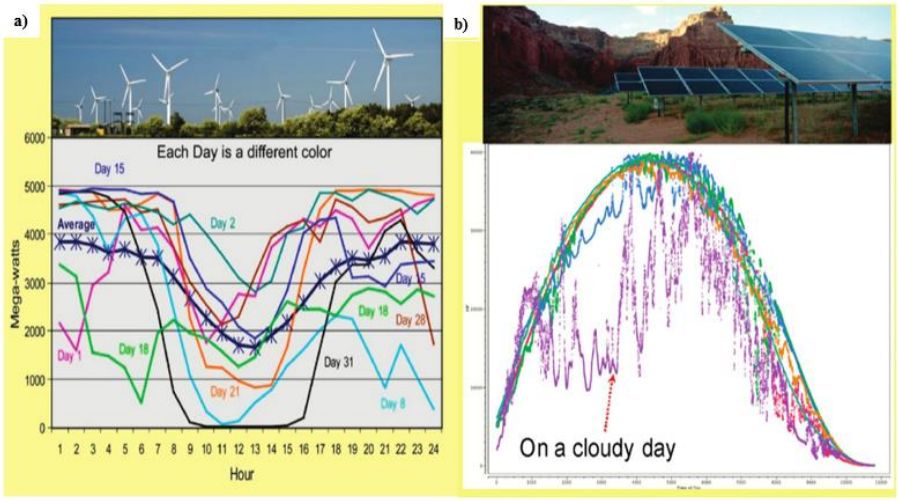

Figure 3. a) Daily profiles of wind power projected by 7x output in April 2005 for the year 2011 in Tehachapi, California, b) 5MW PV power over a span of 6 days in Spain [7]

1.2 Battery energy storage system technologies

ESSs (Energy Storage Systems) can store unused energy from renewable energy by converting the energy into the more conveniently storable form such as mechanical, thermal, chemical energy. Figure 4 shows the possible ESS with the characteristics rated by the power ratings and discharge time for three different application. [8] Compare to other ESSs, the battery is electrochemical energy storage that can be lucrative in the future. The battery has many fascinating features including scalable, flexible power, fast response time, high efficiency, long cycle life and environmentally friendly. Despite the price of the battery which is expensive, however, these advantages are tough to ignore, and the price is soon to be decreased. [8] Among all the batteries, Lithium-ion battery is the most promising battery for the future ESS.

Lithium-ion batteries (LIB) is a battery that uses lithium as a mean to transport electron from anode to cathode. LIB is known to have one of the greatest energy density and power density due to the low ionic radii of Lithium. Furthermore, the Lithium has the highest cell potential due to low reduction potential. [8-9] Thanks to these properties, Lithium-ions batteries has been applied everywhere, from handphone, electric car, to energy grid storage. However, not only LIB cost is still high compared to other ESS (Figure 5), but also the issue of Lithium shortage may happen in the future. [10-11] Thus, research in new material which has similar properties as Lithium, but higher abundance and lower price is needed before the Lithium-ions become extinct.

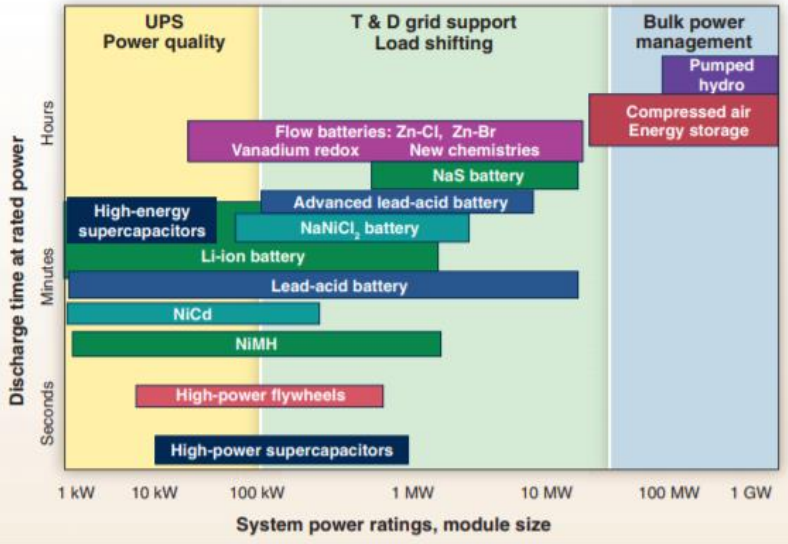

Figure 4. Graph of system power ratings against discharge time of energy storage for three different energy storage application[8]

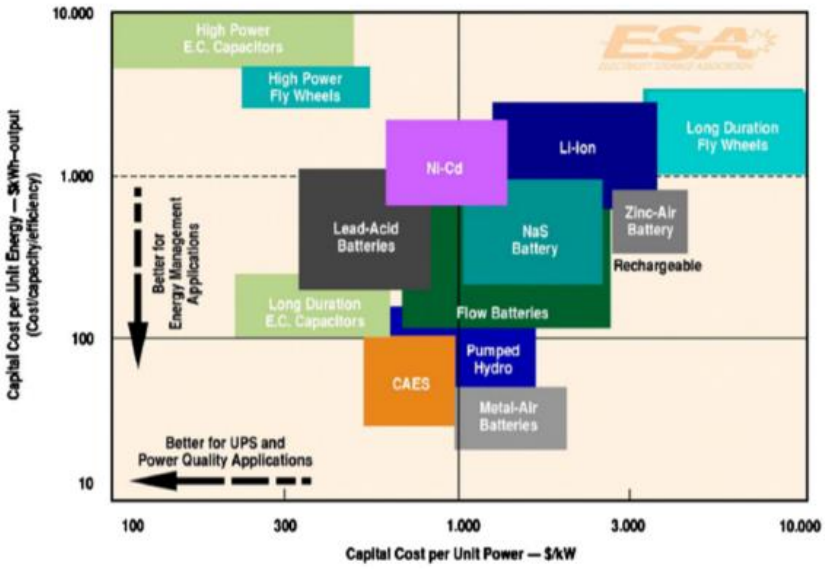

Figure 5. Capital cost per unit power vs Capital cost per unit energy of different energy storage system[10]

One of the alternative solutions for Lithium-ion Batteries is Sodium-ions batteries since Sodium is cheaper, more abundance, and easier to obtain compared to the Lithium (Figure 6a). [12-14] Sodium is located right below Lithium in the periodic table, thus both elements have many similarities in chemical and mechanical properties. [14] Although sodium has a lower energy density than lithium since Sodium has higher weight and volume, the sodium-based battery still comes out cheaper by 12.6% than LIB due to lower cathode price (Figure 6b). The application of Sodium into battery was successful in the molten salt battery by using Sulfur as an anode (Sodium-Sulfur battery, NaS battery), and this battery has been installed.

NaS battery is one of the most popular molten salt battery and has better cost compare to LIB. NaS battery consists of liquid Sodium and Sulfur separated by β"-Alumina solid electrolyte (BASE) (Figure 7). [16] NaS battery operates at a high temperature (300ºC – 350ºC) since the electrode must be in liquid form to operate well. The NaS battery reaction follow the reaction below: [7][16]

$$\text{Cathode: } x\,S + 2\,Na^+ + 2e^- \leftrightarrow Na_2S_x \; (x = 3 \sim 5) \qquad (1)$$

$$\text{Anode: } 2\,Na - 2e^- \leftrightarrow 2\,Na^+ \qquad (2)$$

$$\text{Cell reaction: } 2\,Na^+ + x\,S \leftrightarrow Na_2S_x \; x = 3 \sim 5) \qquad (3)$$

The installation of NaS battery has risen rapidly from 10 MW in 1998 to over 350 MW by 2010, however, NaS battery still needs better safety and performance for commercialization.

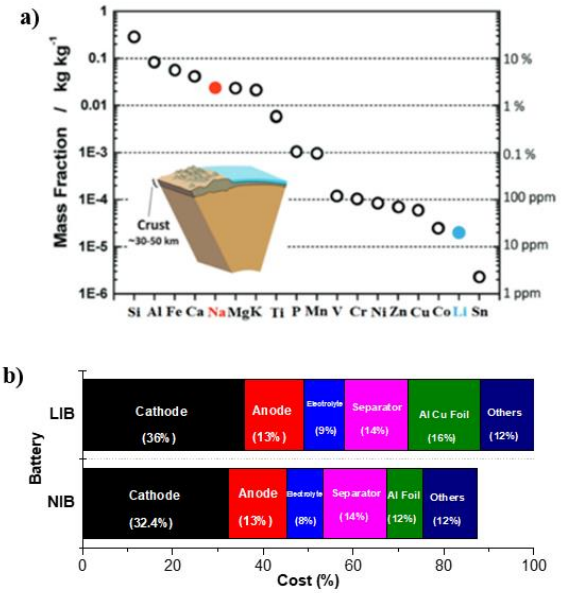

Figure 6. a) The element abundance in the earth, b) comparison between Sodium-ions battery and Lithium-ions battery[12][15]

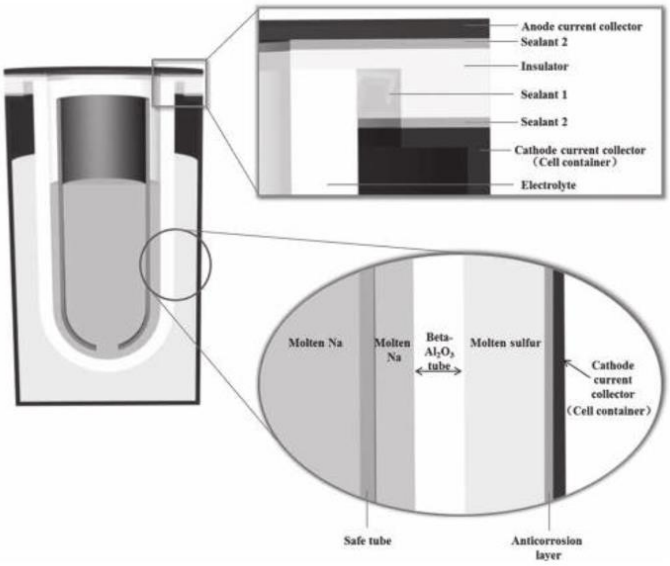

Figure 7. Structure of molten salt NaS battery [16]

1.3. Seawater battery

A novel design of sodium-based battery by harnessing the Sodium-ions inside seawater called seawater battery (Figure 8), was proposed by our group and the battery demonstrate several advantages that NaS and LIB battery do not have, such as low cost, safe, and possible to operate at room temperature. [18] Seawater battery takes advantage of Sodium Chloride salt inside the seawater and uses it to store the energy. This battery uses seawater as a cathode material and possible to cut 30% of the normal price of battery since seawater is free. [15][20] Unlike any conventional battery, the seawater battery can be design without any metal material since the Sodium-ions already exist in the cathode part of the battery. Although there are several drawbacks such as low density and restricted to geography, however, this battery has the potential to be the grid energy storage system in the future. [21]

The reaction in seawater battery starts from Sodium extraction in seawater cathode toward anode as its shown in Figure 9a. During charging, the Sodium-ions move from cathode to anode by passing through the solid electrolyte, and the electrochemical reaction was predicted to follow one of the equation (4 or 5) below. The first reaction (4) results in Oxygen generation and called Oxygen Evolution Reaction (OER), while the second reaction (5) creates Chloride, which also known as Chlorine Evolution Reaction (CER). The first cycle charge voltage was observed to be around 4.05 V, indicating that the reaction is most likely leaning toward CER than OER, even though oxygen is thermodynamically favorable preferable to chlorine. [22]

$$2\ NaCl\ (aq) + H_2O(l) \rightarrow 2\ Na\ (s) + 2\ HCl\ (aq) + \tfrac{1}{2}\ O2\ (g) \qquad E^o = 3.94 \qquad (4)$$

$$2\ NaCl\ (aq) \rightarrow 2\ Na\ (s) + Cl_2\ (g) \qquad E^o = 4.07 \qquad (5)$$

During discharge, the Sodium-ions move from the anode toward the cathode, reducing water, and increasing the seawater pH from 7.8 to 9.2 due to NaOH generation. There are two possible scenarios based on whether the Oxygen inside the seawater is reduced during the process or not. These two processes are described in the equation (6) and (7) below and the voltage shows a contrast difference between both electrochemical reaction. The discharge voltage was proven experimentally around 2.9 V (Figure 9b) and this result shows that the voltage is closer to the reduction with the participation of oxygen. The removal of oxygen can greatly decrease the voltage to 1.9 V, which is similar as equation (7). [22]

$$Na\ (s) + \tfrac{1}{2}\ H_2O + 1/4\ O_2\ (g) \rightarrow NaOH(aq) \qquad E^o = 3.11\ V \qquad (6)$$

$$Na\ (s) + H_2O\ (l) \rightarrow NaOH\ (aq) + \tfrac{1}{2}\ H_2\ (g) \qquad E^o = 1.88\ V \qquad (7)$$

The component of seawater battery consists of cathode current collector, a solid electrolyte, a liquid electrolyte, and an anode component. Firstly, the heat-treated carbon felt is used as cathode current collector since carbon felt has good electrochemical stability, good electronic conductivity, large surface area, hydrophilic if it's heat-treated, and reasonable price. [23] On the anode side, the seawater battery is recorded to use different anodes such as Sodium metal, a hard anode, Antimony sulfide (Sb_2S_3), Tin/carbon (Sn/C) and red phosphorous carbon composite (P/C). [24-27] The electrolytes in seawater battery can be categorized based on its form into two different categories, a liquid electrolyte, and solid electrolyte. The liquid electrolyte used to accelerate the movement of Sodium-ions during charging/ discharging. Two liquid electrolytes which are 1 M $NaClO_4$ and 1 M $NaCF_3SO_3$, is known to be capable in seawater battery. [28] On the other hand, there are two different candidates for the solid electrolyte in seawater battery, β"-Alumina and NASICON. These solid electrolytes will be discussed in the next section. [29]

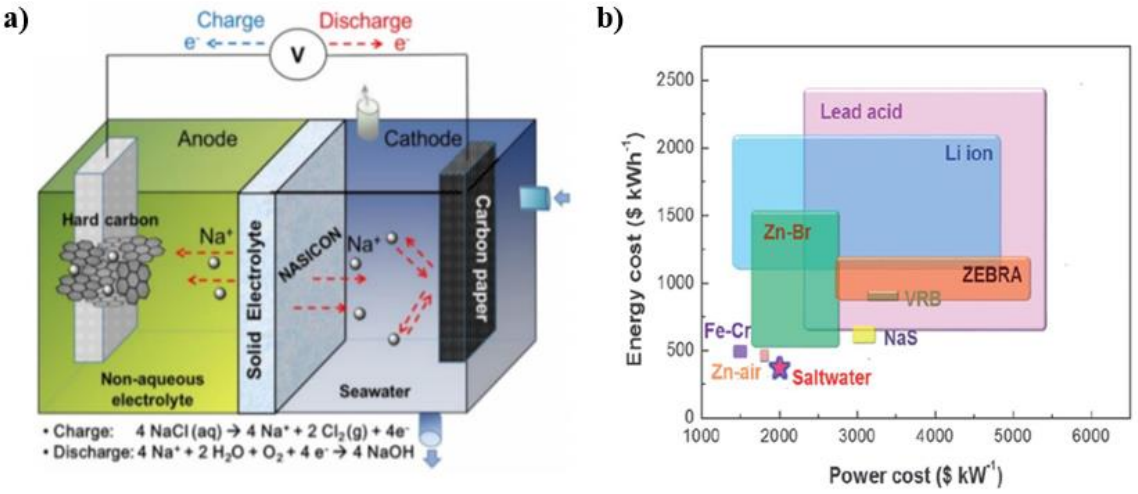

Figure 8. a) The Novel design of seawater battery and b) cost comparison between seawater battery and another type of battery [18]

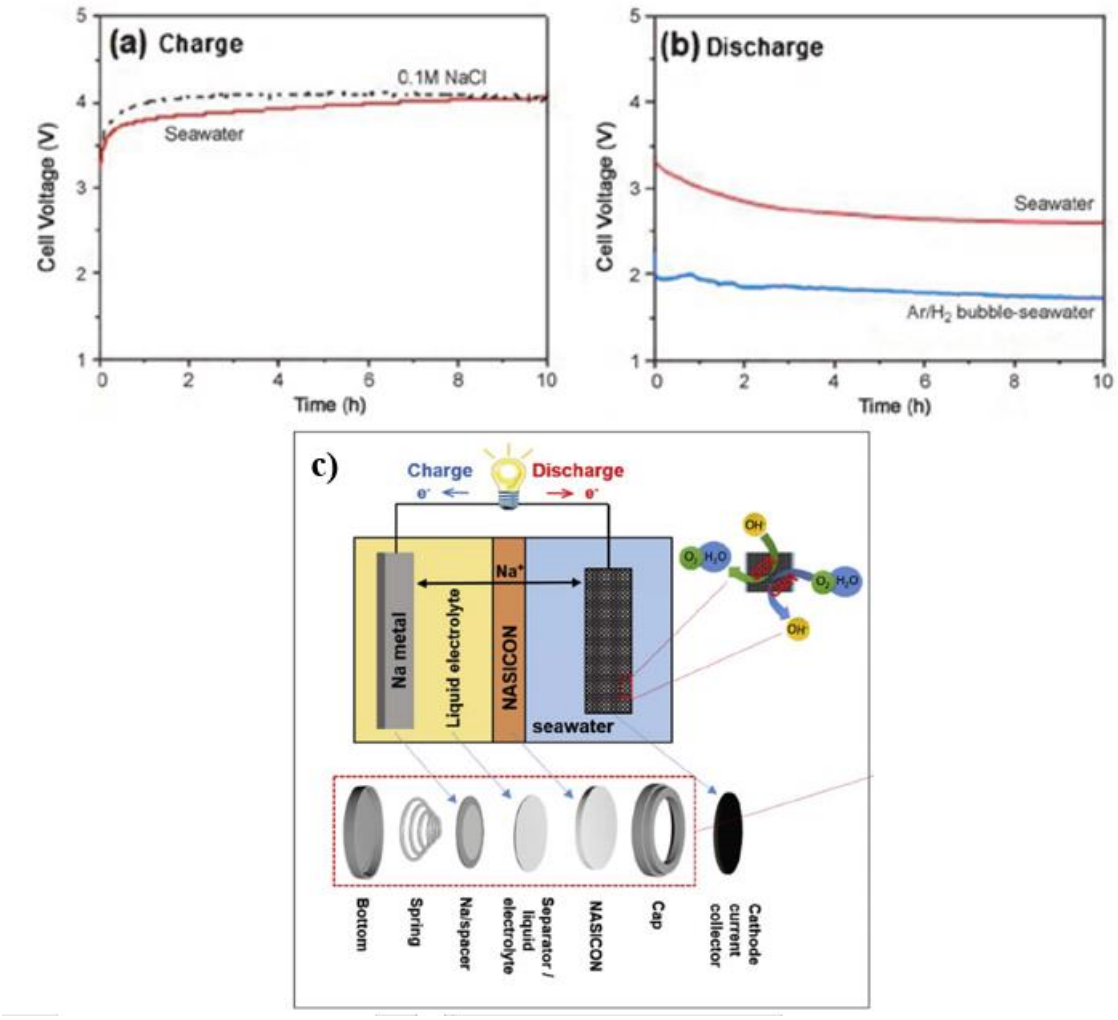

Figure 9. The time vs voltage graph of seawater battery during a) charging and b) discharging, and c) component of coin cell seawater battery [22][23]

1.4. Solid electrolyte in seawater battery

An electrolyte in battery act as an intermediate to separate while promoting the movement of the ions between anode and cathode at the same time. In the conventional battery system, the electrodes are usually in solid form and can be easily separated by the only liquid electrolyte. However, the seawater battery needs a physical barrier to prevent diffusion and direct contact between the liquid cathode (seawater) and solid anode. There are several requirements for a material to be a solid electrolyte. Firstly, the material should have low electronic conductivity, high ionic conductivity at least 10^{-4} S/cm in room temperature and wide electrochemical stability windows. [30] Secondly, the stability of the material in seawater is needed for the battery to have better efficiency in the application. [29] Lastly, the mechanical strength is needed to prevent any leaking and physical contact between electrodes.

Based on the criteria mention above, two materials were already tested already tested and applied to the seawater battery by Yongil et al [29]. The first material is β”-Alumina, which has been applied into several molten salt battery applications. Sodium β”-Alumina is known to have high ionic conductivity (1.0×10^{-3} S/cm) and good mechanical strength, however, Sodium β”-Alumina is not stable against moisture. On the other hand, Na-superionic conductor or known as NASICON ($Na_3Zr_2Si_2PO_{12}$) can be also a good candidate with similar electrochemical properties, but superior stability in water compared to Sodium β”-Alumina. The detail of each material in seawater battery application will be discussed in the next section.

1.4.1 Solid electrolyte candidate: Sodium β”-Alumina

The structure of Sodium β-Alumina was invented in 1916 through the Bayer process and it wasn't applied as an electrolyte, but for industrial furnaces due to great refractory properties. [31,32] The structure of Sodium β-Alumina is two-dimensional crystal with alternative closely-packed layer and the loosely-packed layer where the Sodium-ions stored. The molecular structure of Sodium β-Alumina is 11 Al_2O_3 – 1+x Na_2O (where x is $0 < x < 0.57$). The Sodium-ions can be increased by the addition of Lithium or Magnesium doping from 0.57 to 0.67, which later known as Sodium β”-Alumina. [34] Currently, Sodium β”-Alumina is used for the solid electrolyte in the Na-S battery. [18]

The stacking in Sodium β-Alumina and Sodium β”-Alumina consist of spinel block and conduction plane as shown in Figure 10a. [35] The Sodium-ions exist inside the empty interstitial oxygen site at the loosely-packed layer of both types of Sodium β-Alumina. The conduction pathway of Sodium-ions in Sodium β-Alumina and Sodium β”-Alumina is through the two-dimensional pathway found in the conduction plane (Figure 10b). [36] The difference between Sodium β-Alumina and Sodium β”-Alumina is the small doping by Lithium or Magnesium, resulting in the Frankel defect. This defect leads to additional Sodium-ions, altering the stacking (Figure 11) and crystal structure from hexagonal to rhombohedral. The doping causes the increment in conductivity, thus Sodium β”-Alumina structure is more popular in solid electrolyte application than Sodium β-Alumina. [37]

Sodium β”-Alumina can be a great candidate for solid electrolyte due to high conductivity, low electronic conductivity, good mechanical strength, and chemical passivity. However, Sodium β”-Alumina is not stable against moisture and water can be one fatal disadvantage for the seawater battery application. When Sodium β”-Alumina in contact with water, the water occlusion rapidly occurs while slow hydronium-ion diffusion also happens simultaneously. These reactions leading to higher resistance, lowering the conductivity of Sodium β”-Alumina dramatically. [38] Therefore, the application of Sodium β”-Alumina for seawater battery is unlikely to be successful.

The research on Sodium β”-Alumina application as solid electrolyte seawater battery has been experimented by Yongil et al. [29] The capacity of seawater battery with Sodium β”-Alumina decrease dramatically after 3rd cycle (Figure 12a). Furthermore, the structural change was observed by XRD (Figure 12b) along with ionic conductivity loss after 10 cycles (Figure 12c and Figure 12d). This phenomenon is most likely because of the seawater reaction with Sodium β”-Alumina resulting in water occlusion and hydronium ion diffusion into the crystal lattice. Therefore, Sodium β”-Alumina is not suitable solid electrolyte candidate for seawater battery application due to unstable behavior during contact with water. [29]

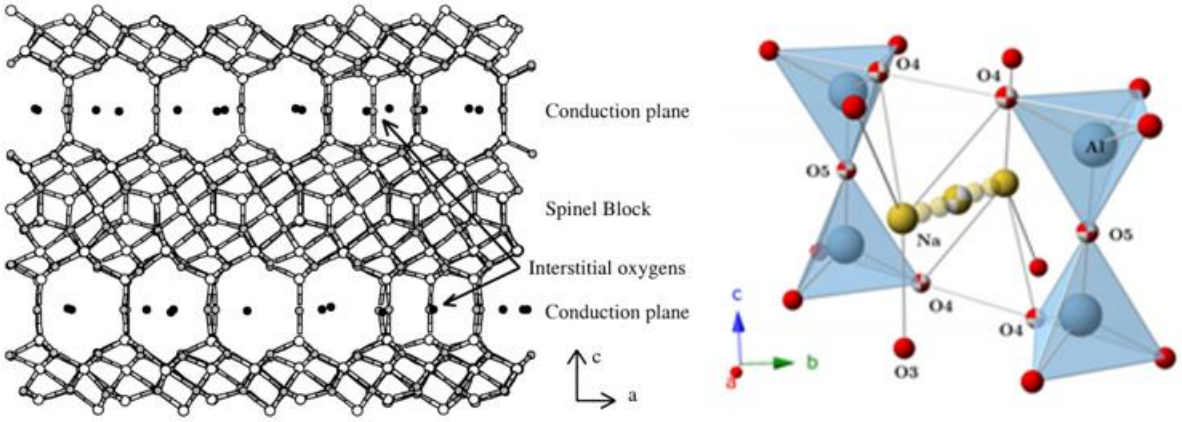

Figure 10. a) Structure of Sodium β-Alumina and b) 2-dimensional conduction pathway of Sodium β-Alumina

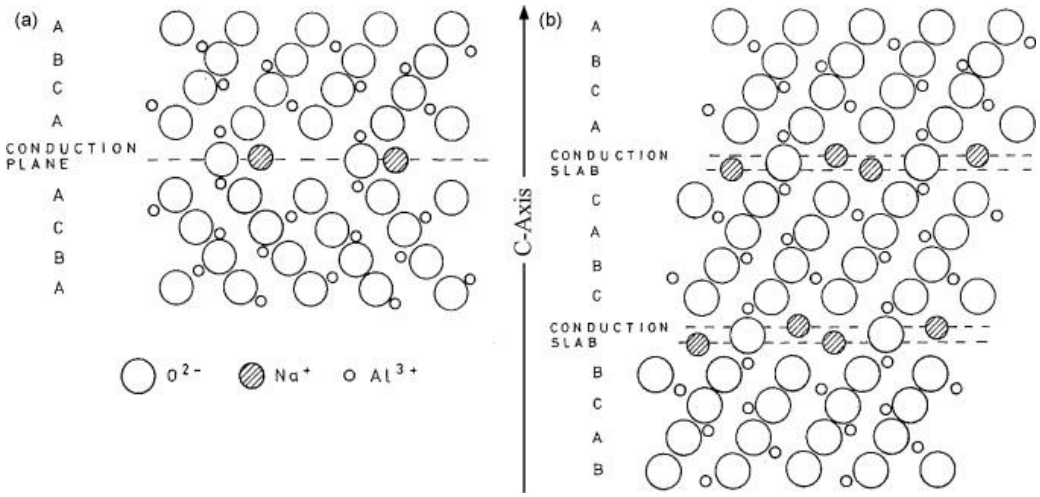

Figure 11. Stacking difference in a) Sodium β-Alumina and b) Sodium β”-Alumina

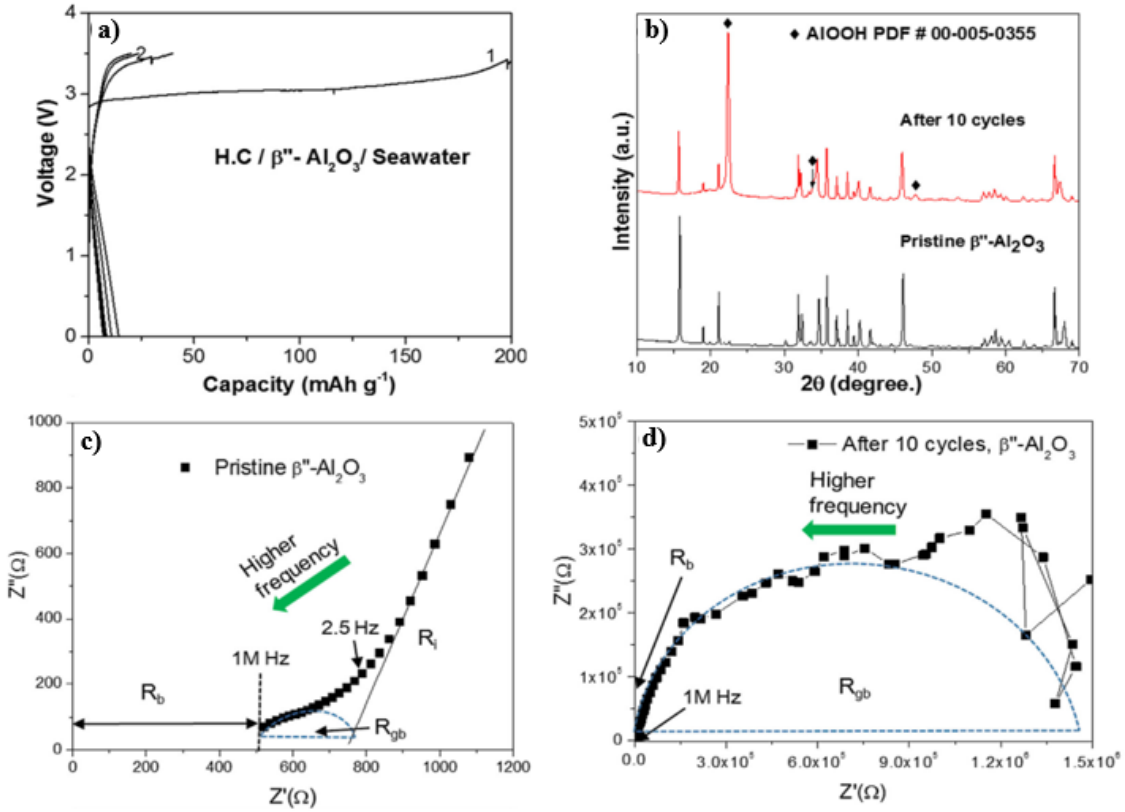

Figure 12. Application of Sodium β”-Alumina in seawater battery application: a) the cycle test, b) Sodium β”-Alumina X-ray diffraction pattern of pristine and after 10th cycles, and Electronic Impedance Spectroscopy of Sodium β”-Alumina a) before (pristine) and d) after 10th cycle [29]

1.4.2 Solid electrolyte candidate: Na^+ Super Ionic Conductor (NASICON)

1.4.2.1. Structure of NASICON

Na Super Ionic Conductor or known as NASICON is another solid electrolyte which has similar properties as Sodium β"-Alumina. NASICON has chemical formula of $Na_{1+x}Zr_2Si_xP_{3-x}O_{12}$ ($0 < x < 3$) and $Na_3Zr_2Si_2PO_{12}$ ($x = 2$) shows the highest conductivity, which is around 10^{-3} S/cm. NASICON is possible to be applied as solid electrolyte not only because of high conductivity, but also small electronic conductivity and good mechanical strength. For seawater battery application, NASICON is more superior than Sodium β"-Alumina since NASICON has better stability in water and moisture. Thus, NASICON predicted to have better capability for the solid electrolyte in seawater battery.

The first family of NASICON was discovered in 1968 by L. O. Hagman and P. Kierkegaard with the formula $NaZr_2P_3O_{12}$ ($x = 0$). The elemental substitution of NZP was studied, however, it was focused on the substitution of Zirconium with the same group element (Titanium and Germanium). The $NaZr_2P_3O_{12}$ was shown to be a rhombohedral structure with the corner of both PO_4 tetrahedral and ZrO_6 octahedral connected to each other. The Sodium-ions was inside the octahedral prism of oxygen linked by PO_4, which is in the middle of two stacked triangular faces of ZrO_6 and create a major structure with the $O_3ZrO_3NaO_3ZrO_3$ arrangement (Figure 13). [39]

On 1976, Hong et al propose a Phosphate substitution with Silicon in $NaZr_2P_3O_{12}$. [41] Upon the substitution with silicon, the additional Sodium-ions balances the charge and a new compound is proposed named Na Super Ionic Conductor (NASICON). The formula of NASICON is $Na_{1+x}Zr_2Si_xP_{3-x}O_{12}$ where x starts from 0 to 3. The additional silicon increases the trigonal bottleneck size between Na (1) to Na (2), which result in ionic conductivity increment. This trend is a peak when $x = 2$ and decrease afterward. NASICON with $1.8 < x < 2.3$ is reported to change the structure from rhombohedral to monoclinic crystal structure. However, later it was known that monoclinic NASICON return to rhombohedral at high temperature. [40-45]

Ionic conductivity is affected by how fast the ions move from one site to another, and it can be correlated with the sodium site in the NASICON structure. NASICON ($Na_3Zr_2Si_2PO_{12}$) has 4 different sodium sites and separated into two different positions called Na (1) and Na (2) at the rhombohedral structure. In the monoclinic structure, the Na (2) position split into two different sites, which are Na (2) and Na (3). The ratio of Na (1), Na (2), Na (3) sites in NASICON is 1:1:2. [45] The ions movement from each site is analyzed and the conduction path of Na1-Na3-Na1 is proven to be active, while Na1-Na2-Na1 is inactive. [46] In addition, the bottleneck between Na (1) and Na (2) is shown to be the highest, thus limiting the conductivity of NASICON. [44] At x higher than 2, the Na (3) sites disappear and NASICON revert to the rhombohedral structure with lower ionic conductivity. [41]

NASICON is a polycrystalline ceramic consist of different phases, and the impure phases are usually called secondary phases. The secondary phase is form in any type of NASICON and the total is higher as more the x (in $Na_xZr_2Si_xP_{1+x}O_{12}$) increase. In the NASICON with formula composed by Hong et al, Zirconium Oxide forms as secondary phase and can be easily detected by XRD (Figure 15a). The crystal can also be easily seen by TEM and observed as a white crystal in SEM (Figure 15 b-d). To eliminate this phase, Von proposed a new formula ($Na_{1+x}Zr_{2-x/3}Si_xP_{3-x}O_{12-2x/3}$) and this NASICON didn't show any Zirconium phase. However, the glassy phase is still detected in both NASICON. This material appears dark in SEM (Figure 15c-d). Both crystal created by Zirconium precipitation during sintering. During Zirconium precipitation, the other precursor reacts with each other, creating amorphous phase in the NASICON grain boundary. [48-57]

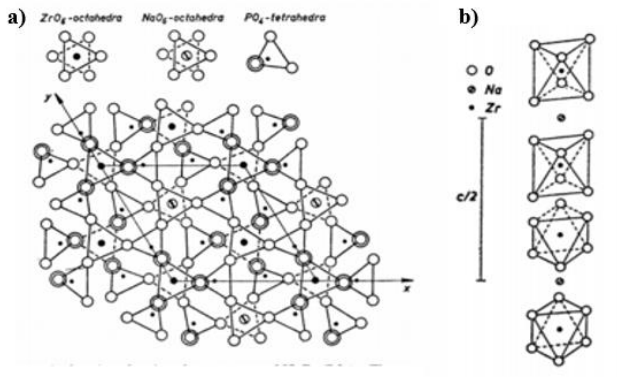

Figure 13. The structure of the first NASICON-type compound, $NaZr_2P_3O_{12}$ a) viewed along [001] and b) Sodium sites in $NaZr_2P_3O_{12}$ [38]

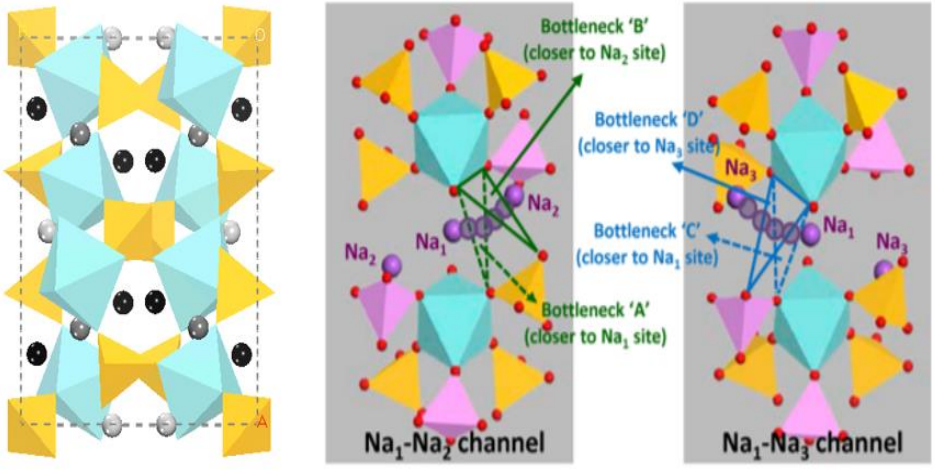

Figure 14. a) NASICON structure and conduction pathways through b) Na1-Na2 Channel and c) Na1-Na3 channel [44]

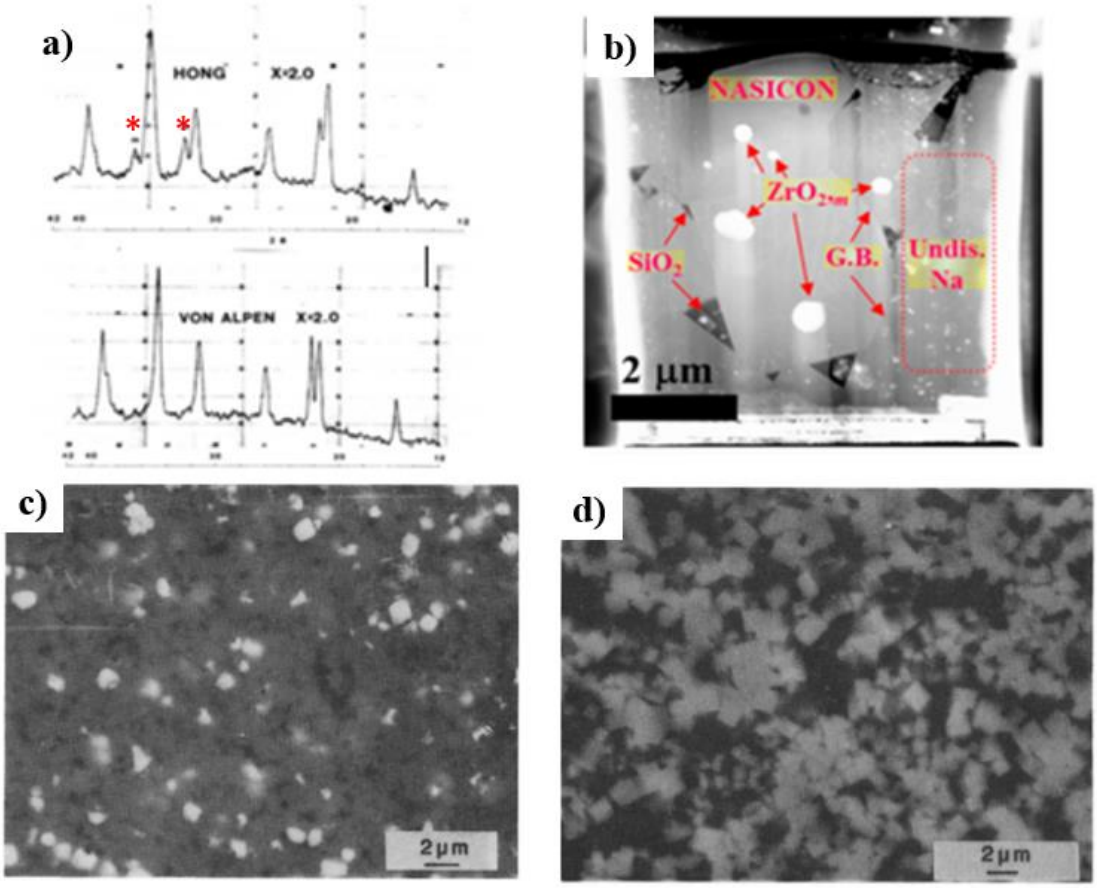

Figure 15. a) Hong-type and Von-type NASICON THROUGH X-ray Diffraction, b) TEM of Hong-type NASICON, and SEM image of c) Hong-type and d) Von-type NASICON [48][59]

1.4.2.2. NASICON stability in water

NASICON has better stability against water and moisture compared to β”-Alumina. Although NASICON doesn't react as quickly as β”-Alumina, however, NASICON is known to be reactive with water. Two different mechanisms of NASICON reaction with water was observed. The first reaction is through the dissolution of the second phase in polycrystalline NASICON. The dissolution is unavoidable once NASICON in contact with water or aqueous solution regardless of the condition. The other reaction is hydronium exchange which sodium inside the NASICON replaced by Hydronium-ions.

The influence of water in NASICON was analyzed in 1984 by immersing NASICON in the water at room temperature. During the immersion, there are no observable properties except the increment of the solution's pH. The pH rises higher as the Silicon doping increase (x increase). [48] To proof the change comes from the secondary phase, NASICON with low purity and observable Na_3PO_4 by XRD is immersed in D.I. water. After the immersion, the XRD was analyzed and the Na3PO4 was gone. The loss of high impurity NASICON also accompanies with higher pH increment than low impurity NASICON immersion. [48][57]

The secondary phase can be separated into the zirconia phase and glassy phase which consist of Sodium, Silicon, and Phosphate, and the solubility depend on the acidity of the solution. Sodium and Phosphate secondary phase will dissolve in any condition. Another phase like Zirconium oxide doesn't dissolve in basic or neutral, but only in a strong acid condition. On the other hand, Silicon phase has better solubility in basic condition. Although secondary phase dissolution changes the pH greatly, however, the properties of NASICON is not affected greatly by dissolution. [58]

The other reaction that happens in NASICON is hydronium exchange reaction between hydronium ions in the water and Sodium inside NASICON. This reaction is known to be destructive and can alter the NASICON properties greatly. This reaction was observed at 60^{o}C by R.O. Fuentes, but older study hinted by Ahmad et al [48] hinted that NASICON is unstable at a temperature above 35^{o}C. A study by R.O. Fuentes et al [55] observed the new XRD peak at 18^{o}, 27^{o}, and 35^{o} which corresponds with hydronium NASICON created from the NASICON exchange with HCl by P.G.Komorowski et al. [62] NASICON immersion at high-temperature D.I. water is reported to have poor physical and crack may arise from the replacement due to larger Hydronium-ion size compare to Sodium. Furthermore, the NASICON resistance increases dramatically resulting in lower ionic conductivity. [55] Thus, Hydronium exchange reaction is destructive and may hinder the application of NASICON as a solid electrolyte in the long-term application.

Seawater has natural ions compare to water and might possibly affect NASICON in a different way. Seawater is an aqueous solution that dominated by Sodium, Chloride, Magnesium, Potassium, Carbonate and other natural ions which mention in the table below. [61] The room temperature immersion in seawater has been done for 60 days and it was reported that the intensity at 18° was decreased. However, there is no Hydronium peak observed. The decrement might represent hydronium exchange reaction in NASICON. Another research also was done in seawater at room temperature and high temperature, and surprisingly the chloride penetration is much worse than hydronium ions. [62]

The NASICON was applied as a solid electrolyte in the seawater battery system. The application used Sodium anode, $NaCF_3SO_3$ as liquid electrolyte, and carbon felt for cathode current collector. NASICON solid electrolyte seawater battery. NASICON perform much better as a solid electrolyte in seawater battery system and still retain 91% capacity after 20 cycles. The structure of NASICON is analyzed before and after cycles by XRD and no new peak or defect even after 100 cycles. On the other hand, the ionic conductivity is slightly decreased, but still, maintain at 10^{-3} S/cm. Therefore, NASICON is proven to be applicable as solid electrolyte candidate of seawater battery application for a short period of time. [29]

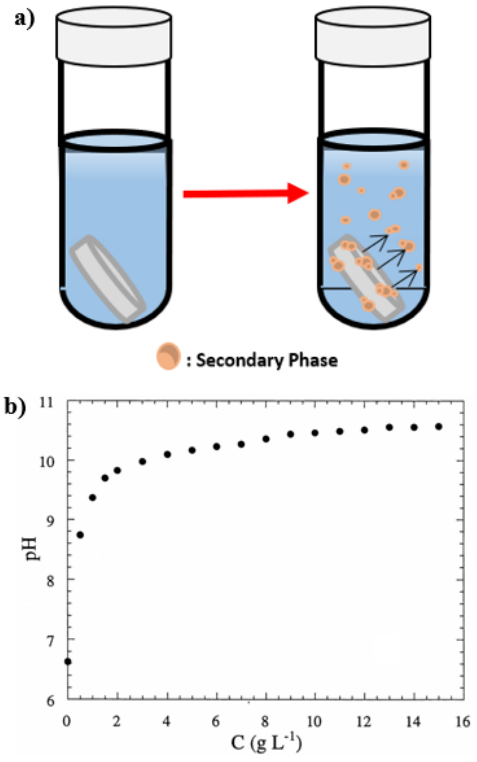

Figure 16. a) Scheme of secondary phase dissolution in aqueous solution, b) pH change in solution after NASICON immersion [57]

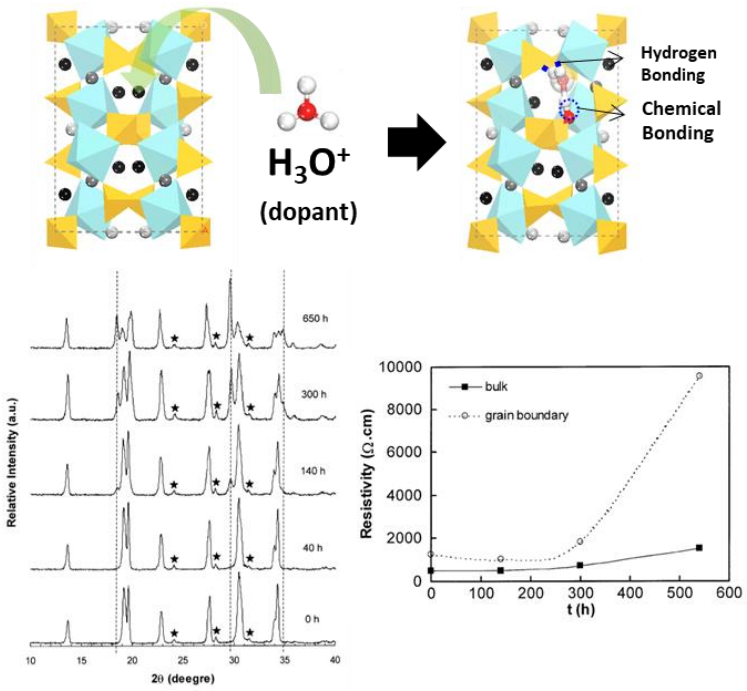

Figure 17. a) Scheme of secondary phase dissolution in aqueous solution, b) pH change in solution after NASICON immersion [55]

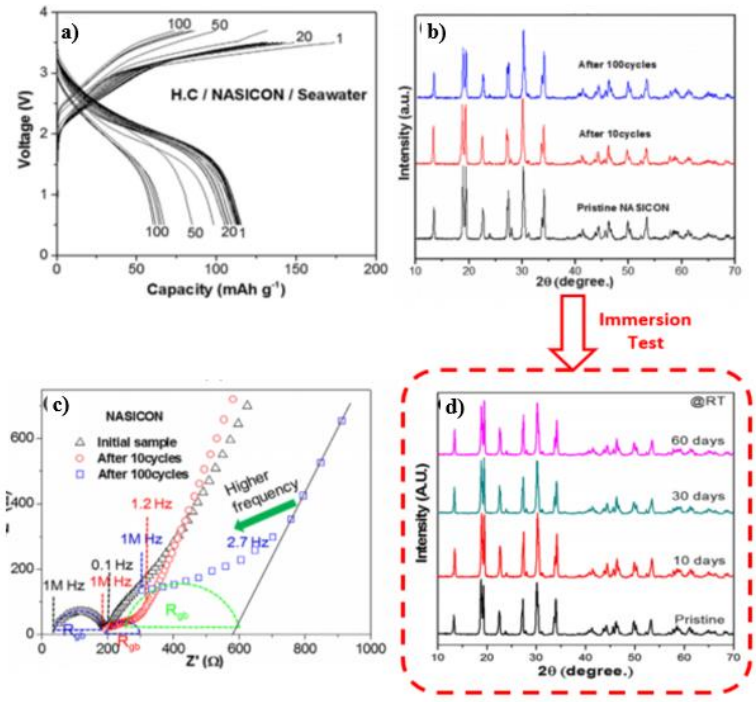

Figure 18. a) Scheme of secondary phase dissolution in aqueous solution, b) pH change in solution after NASICON immersion [29]

1.5 Research purpose

The lifetime of energy storage is one of the most important characteristics when choosing the energy storage system for renewable energy. The longer lifetime of a battery, the lower life cost of the battery itself. Seawater battery has a solid electrolyte that prevents from direct contact between anode and cathode. Any kind of defect in a solid electrolyte such as crack and hole can be fatal for seawater battery since these defects can create short-circuit battery and destroy the battery. In addition, the ionic conductivity should be high to support ion transportation. If the Ionic conductivity decrease, therefore the seawater battery will have lower performance, or even will not charge. One of the reasons that NASICON change is because of the reaction with an aqueous solution. Thus, ensuring the stability of NASICON in room temperature seawater become the main priority before the application in seawater battery. [31]

NASICON is known to react at with aqueous solution by secondary phase dissolution and hydronium exchange happen. Firstly, the secondary phase dissolution happens as the NASICON in contact with water, however, there are no reported properties change after the reaction. On the other hand, Hydronium exchange reaction is destructive at either acidic condition or high-temperature condition, but at room temperature D.I. water is still unknown. Furthermore, there are small pieces of information in NASICON immersion at room temperature for long period (> 3 months). Thus, the NASICON stability in seawater is still unknown and need to research further. [29][47][55][57]

The purpose of this study is to confirm whether NASICON is stable in seawater at room temperature in a longer period (> 3 months). To check the stability, this study immersed NASICON in seawater and other aqueous solution (salt and D.I. water). The difference between them will be analyzed if any and compare with the reference available by the previous research. The result will be a good compass to decide whether the NASICON need to be reinforced or not. If the result is stable, then the focus of the future research will be to test the stability in seawater battery or improving the NASICON properties. However, if NASICON is unstable, the result can be a reference on how to prevent the reaction from happening. This study also gives useful information on where and which change that happens to NASICON over time for easier reinforcement.

2. Experimental Method

2.1 Fabrication of NASICON

A Hong-type Na superionic conductor (NASICON, $Na_{1+x}Zr_2Si_xP_{3-x}O_{12}$) ceramic with x = 2 is fabricated by using solid-state reaction and the procedure is shown in Figure 19a. The starting precursor consists of SiO_2, ZrO_2, and Na_3PO_4. 12 H_2O was weighted based on the $Na_3Zr_2Si_2PO_{12}$ composition and mixed in ethanol. The mixed solution is dried in an oven at 80°C before the calcination started. The dried solution is ground and calcinated at 1100°C in Zirconia crucible overnight and ground after calcination to obtain a fine powder. Around 1 gram of calcinated powder was weight and pressed into NASICON with diameter 1 cm. The pressed NASICON pellet is sintered at 1250°C overnight and the NASICON pellet is formed. The fabricated pristine NASICON pellet will be characterized (refer to instrumental analysis) and immersed in aqueous solution.

2.2 Immersion of NASICON

The sintered pristine NASICON is immersed in water and seawater for a long period of time (> 1 year) at room temperature. The composition of ions in seawater is written in Table 1. A glass jar was used to prevent any unwanted reaction and to observe the NASICON easier from the outside. The previous research shows that the saturation of NASICON is around 4 g./l, but the pH of NASICON still shows a steady rise until 9 g/L. [57] Since the small volume of solution will be taken for further analysis, approximately 1 gram of NASICON per 100 ml of water is prepared for the immersion test. The ratio is always the same regardless of the NASICON form (pellet or powder). To proof the effect of the temperature, the NASICON immersed in the solution at a high temperature. NASICON also immersed in the different salt solution for confirming the effect of ions in the aqueous solution toward NASICON. The immersed NASICON was taken out after a certain amount of time, washed with D.I. water and dried overnight. The overall step of the immersion test is summarized in Figure 19b.

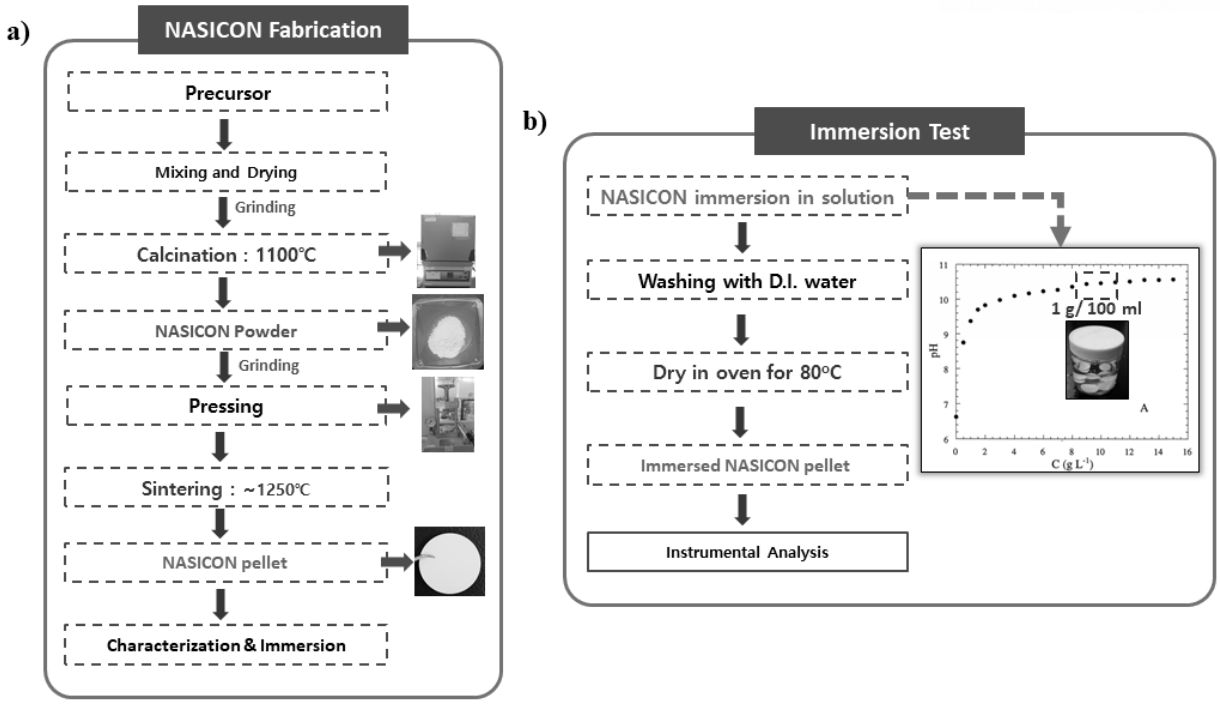

Figure 19. a) The procedure of Hong-type NASICON fabrication and b) experimental plan of NASICON immersion experiments [57]

Cations	Conc. (mg/Kg)	Anions	Conc. (mg/Kg)
Na	10752	Cl	19345
Mg	1295	SO_4	2701
Cations	416	HCO_3	145
K	390	Br	66
Sr	13	BO_3	27

Table 1. Cation and Anion Composition in Seawater

2.3 Instrumental analysis

2.3.1 Solution analysis

10 ml of immersed solution (D.I. water and seawater) after 5, 15, and 30 days are transferred into the glass vial and the solution is analyzed further by pH and ICP. The pH was recorded by pH meter (Orion Star A211) and the solution was analyzed by Ionic Chromatography Plasma Optical Emission Spectroscopy (ICP-OES, Varian 700-ES). The secondary phase cations such as Zirconium, Silicon, and Phosphate are analyzed, and the dissolution of these cations are measured in milligram per liter (Figure 20).

2.3.2 Structural and surface Morphology Analysis

NASICON crystal structure of the sintered and immersed materials were analyzed by using X-ray diffraction (XRD, Bruker AXS D8 Advance) with Cu Kα radiation. The XRD scan range was set up from 10^{o}-40^{o} with step size 0.0346^{o}. To proof, the Hydronium-ions sticking on the surface of NASICON, depth profiling by using TOF-SIMS (ION TOF, TOF-SIMS 5) and the procedure is like the report by Jae-il Jung et al. [59]

The surface of NASICON is taken by Secondary Electron Microscopy (SEM, FEI Quanta 200FEG and FEI Verios 460) and both types of equipment provide Backscattered Electron (BSE-SEM) and Energy Dispersive X-ray. The beam voltage was set up to 10 kV and calibrated to take a clear image of surface NASICON. For a better image, the NASICON is ion milled (Hitachi IM4000+) and the phases can be clearly differentiated by using BSE-SEM. Semi-quantitative composition analysis is taken by using EDX at different phases in NASICON. The cross-section of NASICON pellet is further process by FIB (Helios NanoLab 450, FEI) for Transmission Electron microscopy (TEM, JEM-2100F JEOL) analysis. The TEM is operated at 200 kV and the EDS (Aztec, Oxford) and EELS were taken for further analysis (Figure 20).

2.3.3 Mechanical and Electrochemical Properties

A small circle with the diameter of 1 cm on both sides of NASICON surface is coated by platinum at 20 mA for 120 seconds by using Pt-Sputter (FEI sputter, Tuscan Emitech K575X). The resistance of NASICON is analyzed by using Electron Impedance Spectroscopy (EIS, Biological VSP 300). EIS spectra jobs. From the impedance test, grain resistance and grain boundary resistance can be obtained by the X-intercepts of the semi-circle. At room temperature, the grain boundary dictated the conductivity of NASICON, therefore the ionic conductivity is calculated by using the formula below.

$$Ionic\ Conductivity\ (S/cm) = \frac{1}{R_{grain\ boundary}} \times \frac{Thickness}{Sputtered\ Area} \qquad (8)$$

The mechanical strength of NASICON is obtained by using the Vicker hardness test (Figure 20). At least 9 indentation point is taken at pressure 1 Kg/mm for the accurate hardness analysis. The pressed NASICON was observed by using Optical Microscopy (Machine) and the length of the diamond is measured. The average of each line was taken from the diamonds shaped hole and converted into the hardness by the equation written below: [68]

$$Hardness\ (Hv) = \frac{2\,P\left(\frac{136^{O}}{2}\right)}{d^{2}} = 1854.4\ \frac{P}{d^{2}} \quad (9)$$

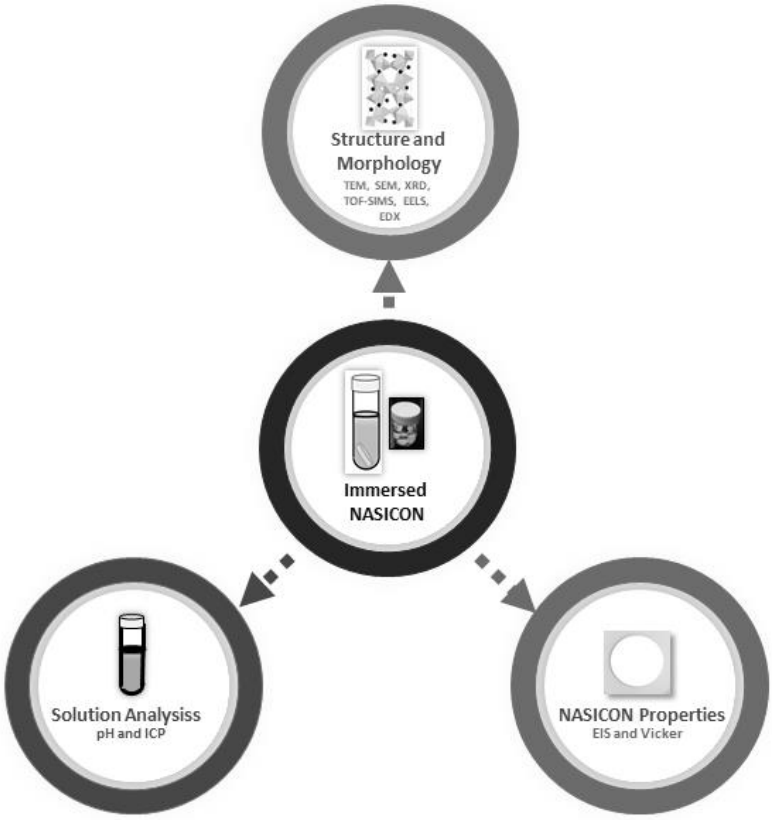

Figure 20. Schematic of NASICON and immersed NASICON instrumental analysis

3. Result and Discussion

3.1 NASICON characterization

The Hong-type NASICON is successfully fabricated and the structure was analyzed by using X-ray diffraction as shown in Figure 21a. The fabricated NASICON shows similar peak as monoclinic NASICON reference, however, an impurity peaks observed at 28.2° and 31.5°. This peak corresponds to the Zirconium oxide peak, which can be found in NASICON as a secondary phase. [48] Three important regions in X-ray diffraction is reported to change by hydronium exchange reaction and these regions will be focused in the analysis (Figure 21b). [55] In the first region (17.5°-21.5°), three peaks were observed (19.1°, 19.3°, and 19.6°) with the first peak is dominant followed by the last peak. This region will be the most important region in this report because this region suffered the most from hydronium exchange reaction. The second region is dominated by one huge peak at 30.5° and a small one at around 30.7°. the huge peak will fall as the Hydronium NASICON arise. Lastly, the third region with two peaks (34.0° and 34.3°) with minor but noticeable change upon the Hydronium substitution dominated the sample. The study of X-ray diffraction pattern will be the main priority of this report on understanding the structural change due to Hydronium exchange reaction.

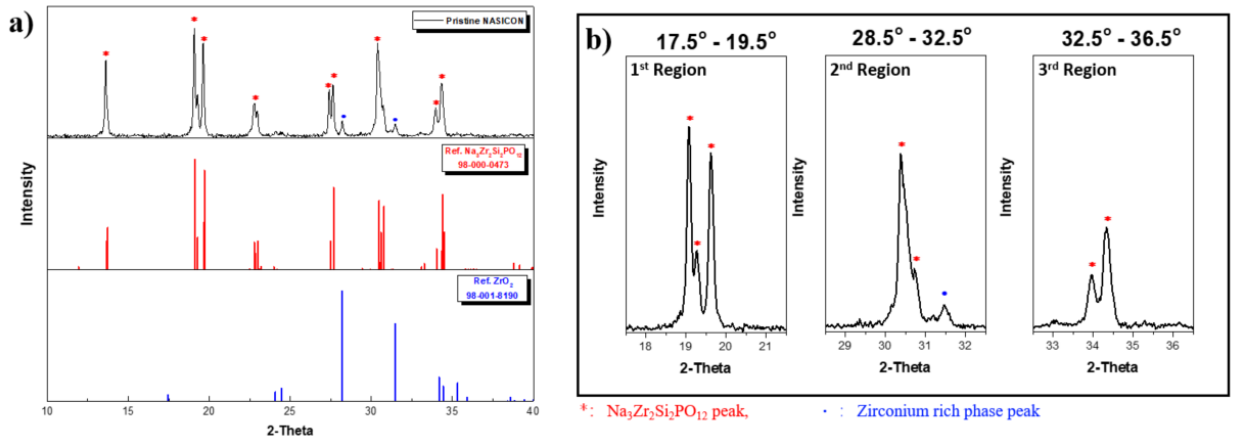

Figure 21. a) The fabricated NASICON ($Na_3Zr_2Si_2PO_{12}$) X-ray diffraction and comparison with the corresponding monoclinic NASICON reference and Zirconium rich phase, and b) three important regions at 17.5° – 19.5°, 28.5° – 32.5°, and 32.5° – 36.5° that will be the key in determining Hydronium exchange reaction

The surface SEM image of NASICON (Figure 22a) is taken and the fabricated NASICON mostly consists of cubic structure. The SEM cross-section (Figure 22b) confirm that there is no surface morphology between the surface and the inner part of NASICON, indicating that NASICON is evenly distributed. To further analyzed the NASICON surface composition, the cross section is ion-milled and Backscattered SEM (BSE-SEM) and EDX are taken from the ion-milled sample. Figure 23a shows the ion-milled NASICON cross-section in the BSE mode and the different color is confirmed. This color difference is related to the molecular weight of the phase (denser phase, brighter color). Based on Figure 23a, there are three different phases which located in the cubic of grain NASICON (grey color), white crystal, and grain boundary (black color). To understand further, the EDX is taken and shows that each phase has different peak intensity which later will be quantified to find the atomic percentage of these phases (Figure 23 b-e). The quantified version (Figure 23e) observed high Zirconium atomic percentage in white crystal region, but low in the grain boundary. However, the silicon shows the exact opposite pattern than Zirconium-ions. This pattern is understandable since the Zirconium was expelled during sintering while the other unreacted precursor formed amorphous phase region in the grain boundary. [48]

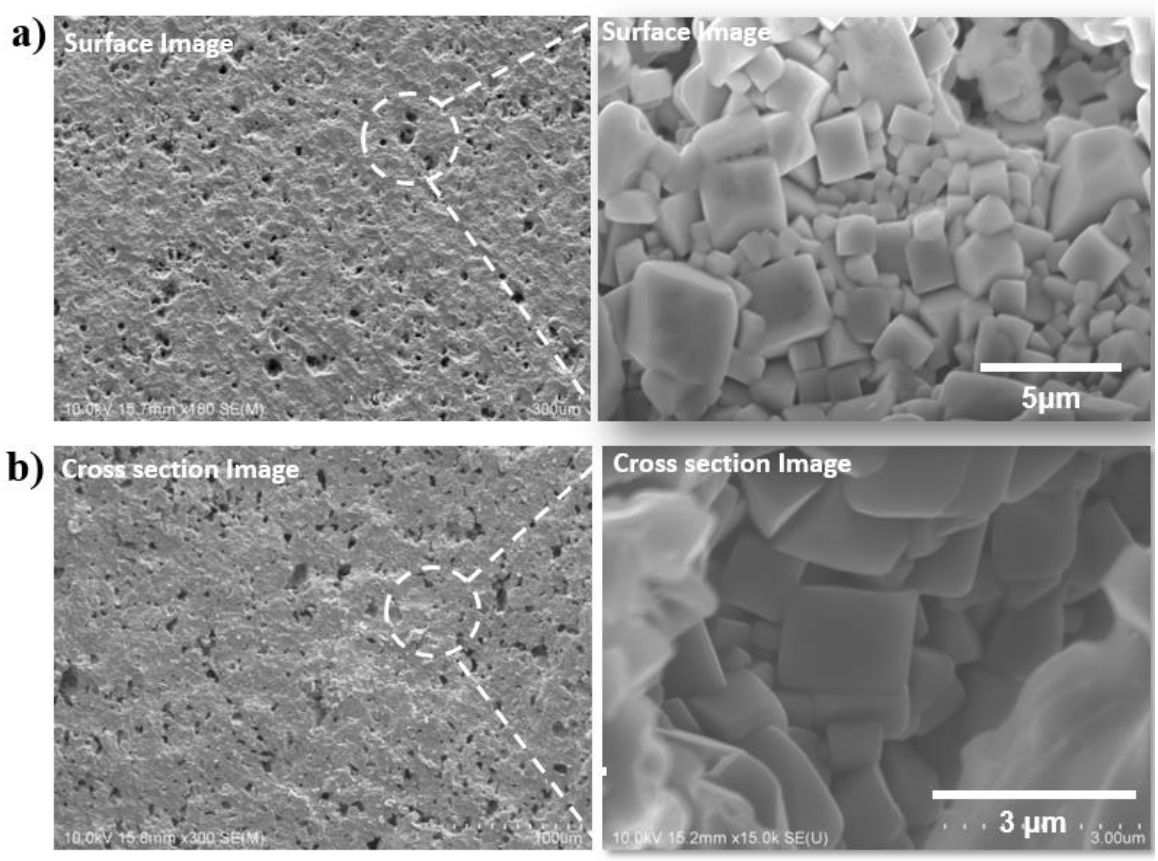

Figure 22. The SEM image of a) the surface and b) the inner morphology of fabricated NASICON pellet at low and high magnification

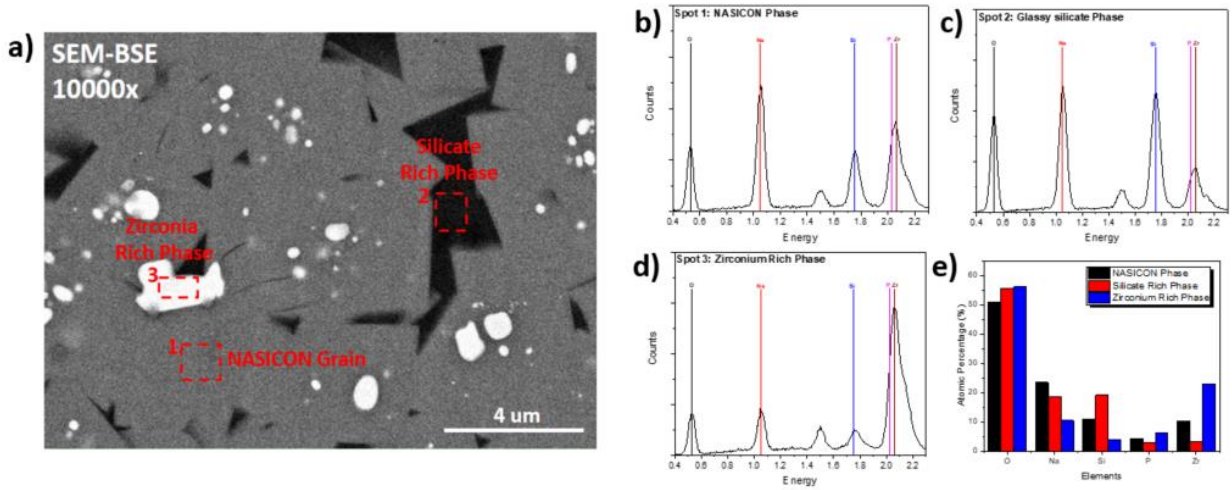

Figure 23. a) The Backscattered Electron SEM (BSE-SEM) image of Ion-milled cross section NASICON and the EDX peak of b) grain NASICON phase, c) amorphous silicate-rich phase, d) Zirconium rich phase and e) the quantified comparison of these peaks.

The surface analysis of NASICON is further analyzed by using TEM. After high magnification of NASICON grain, the NASICON is observed to be polycrystalline structure since the crystal is randomly arranged (Figure 24). On the other hand, the crystal arranged perfectly in the white crystal which later confirmed by EDX as Zirconium rich phase (Figure 25). The grain boundary (Figure 26) is dominated by silicon and fewer Zirconium-ions existed in that region. To understand the composition of NASICON, the TEM area measurement is taken and the NASICON composed of 84.7% NASICON phase, 3% Zirconium phase, 9.9% silicate-rich phase, and 1% of others. This result has higher silicon content than the reference by Jae-Il Jung et al [59], but a similar quantity of NASICON grain phase (Figure 27).

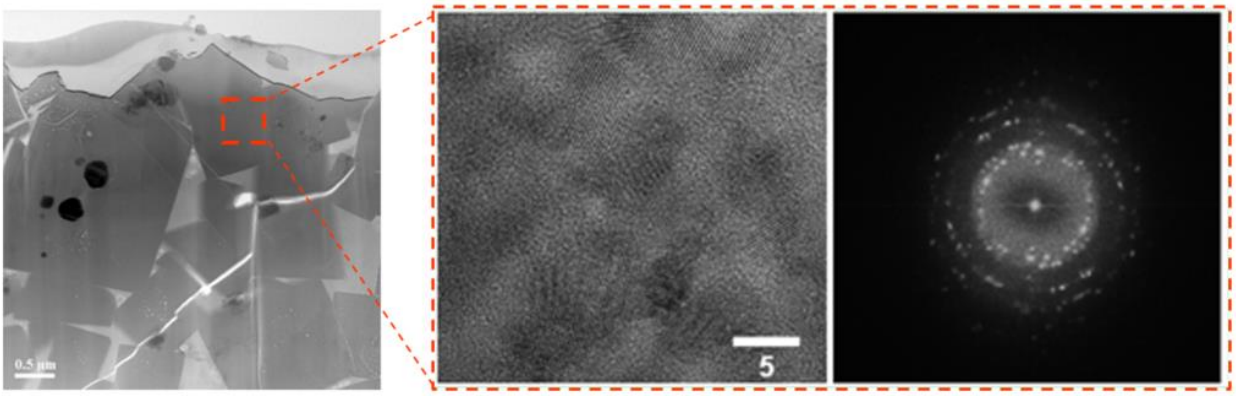

Figure 24. TEM result of Pristine NASICON and high magnification of polycrystalline NASICON

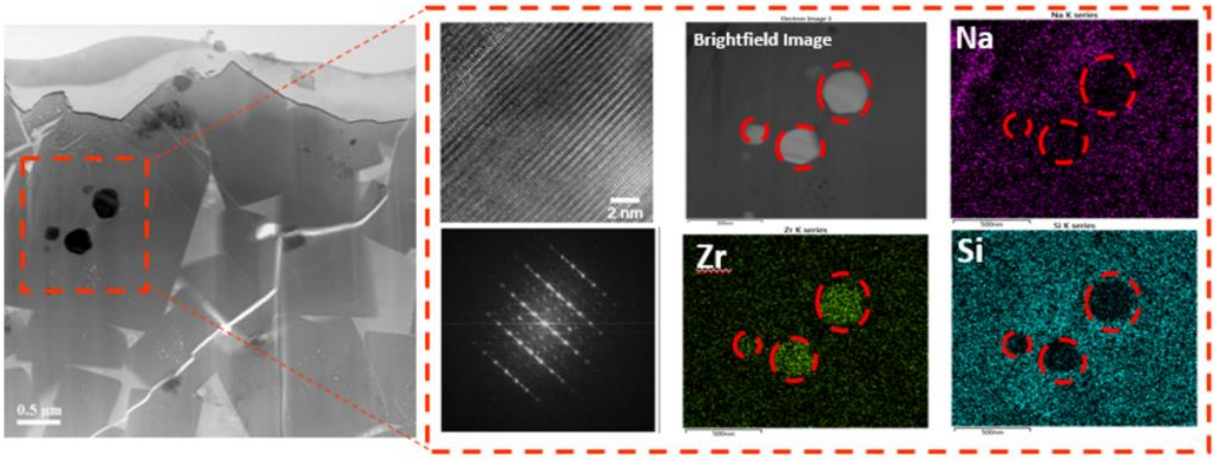

Figure 25. TEM result of Pristine NASICON, high magnification, and EDX comparison of Zirconium rich phase

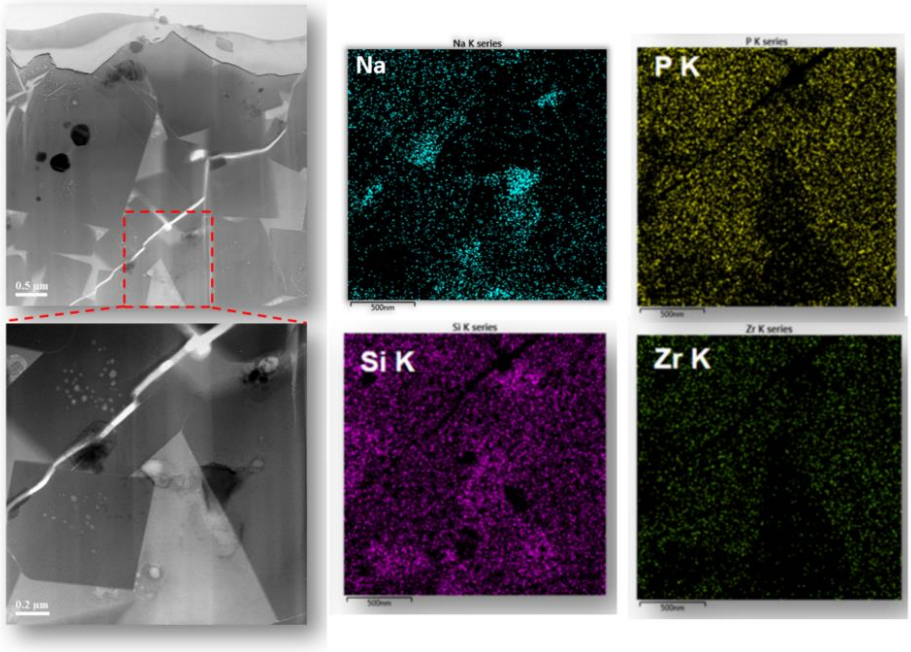

Figure 26. TEM result of Pristine NASICON, high magnification, and EDX comparison of Silicate rich phase (grain boundary)

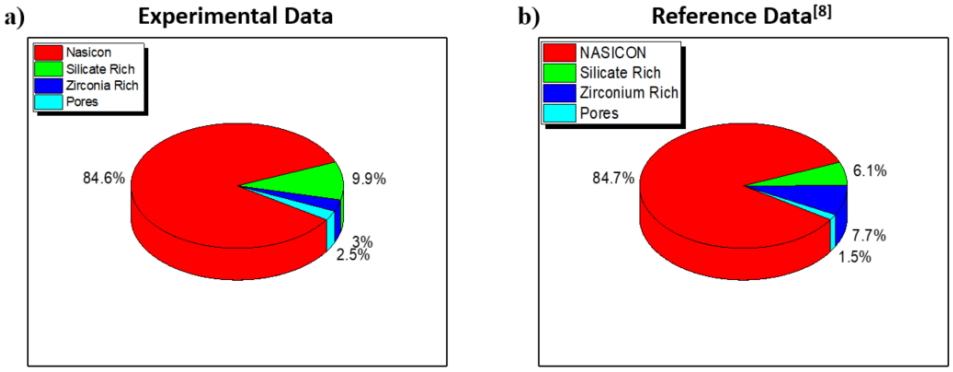

Figure 27. TEM area measurement of the a) fabricated pristine NASICON and b) reference by Jung-Il Jung et al [59]

The electrochemical properties and mechanical properties of NASICON is studied through Electron Impedance Spectroscopy (EIS) and Vicker hardness test. Figure 28a shows the semi-circle graph of EIS result for NASICON conductivity analysis. Two different resistance can be derived by the two x-intercepts through circle fit, which related to the resistance of NASICON grain at lower x-intercepts and NASICON grain boundary at the other. At low temperature, the grain boundary decreased the conductivity of NASICON bulk, thus the conductivity will be converted by using the grain boundary resistance. [60] By using the formula written in the experimental method section, the ionic conductivity of the fabricated NASICON shows 6.9 x 10^{-4} S/cm. The mechanical property is also analyzed, and a diamond was observed after the pressing (Figure 28b). The vertical and horizontal sides of multiple diamonds are measured, and the average length of the sides is converted into the hardness based on the formula mention previously and the pristine NASICON shows the hardness around 331 Hv.

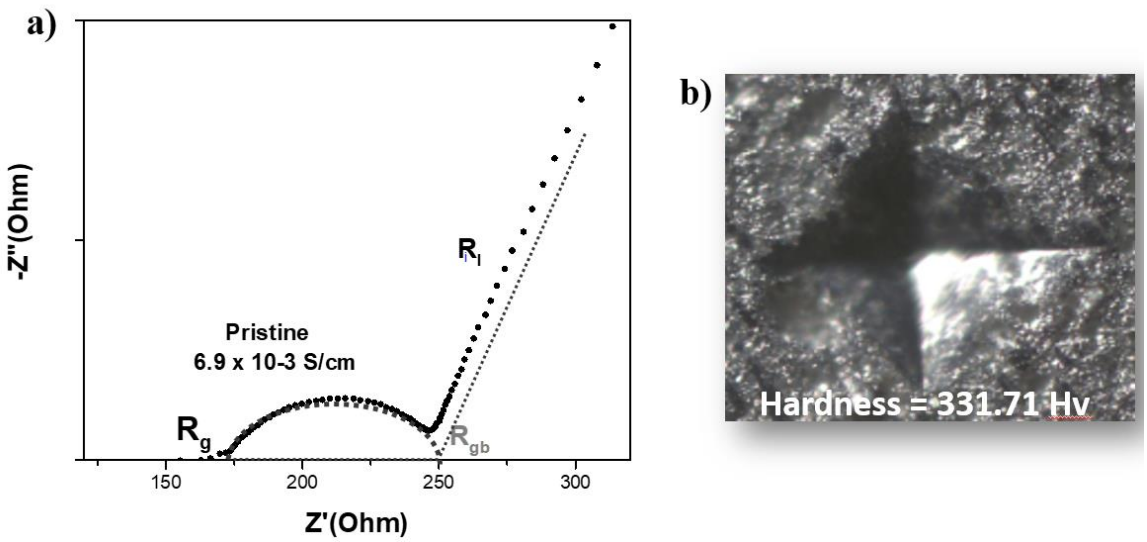

Figure 28. a) The EIS and b) Vicker hardness test result of pristine NASICON

3.2 Secondary phase dissolution

NASICON is a polycrystalline crystal and consist of multiple phases such as Zirconium rich phase and Silicate rich phase. During immersion in the aqueous solution, these phases might dissolve regardless of the condition. This dissolution is difficult to measure by NASICON analysis, but possible through solution analysis which can be obtained from the solution in immersed NASICON. Figure 29a shows the pH result of NASICON immersion in room temperature after certain times and the pH change can only be observed in D.I. water immersion, but not seawater. The pH increased and peaked after 15 days immersion at around pH 9.5 in D.I. water. Surprisingly, the pH in seawater immersion is stable at around pH 8. The pH increment comes from the ions of NASICON secondary phase dissolution. The ions contained in the solution after immersion is analyzed further by using Inductively Coupled Plasma Optical Emission Spectroscopy (ICP-OES).

ICP-OES can measure the cations of the secondary phase dissolution and there are three possible cations that correlated with secondary phase dissolution (Zirconium, Silicon, and Phosphate). Figure 29b-d shows the ICP result of NASICON immersion in D.I. water and seawater after 5, 15, and 30 days. Based on this result, the Zirconium didn't dissolve in both seawater and D.I. water since Zirconium has low solubility in aqueous solution. On the other hand, other ions such as Silicon and Phosphate dissolve more in D.I. water than seawater (Figure 25d). At 15 days, the dissolution of Silicon in seawater is slightly higher than Phosphate since Silicon tends to dissolve more in basic solution. [58] The dissolution didn't increase after 15 days immersion because the immersed solution reaches the saturation point at 15 days as shown in pH result (Figure 25a). This phenomenon might be the effect of natural ions inside the seawater.

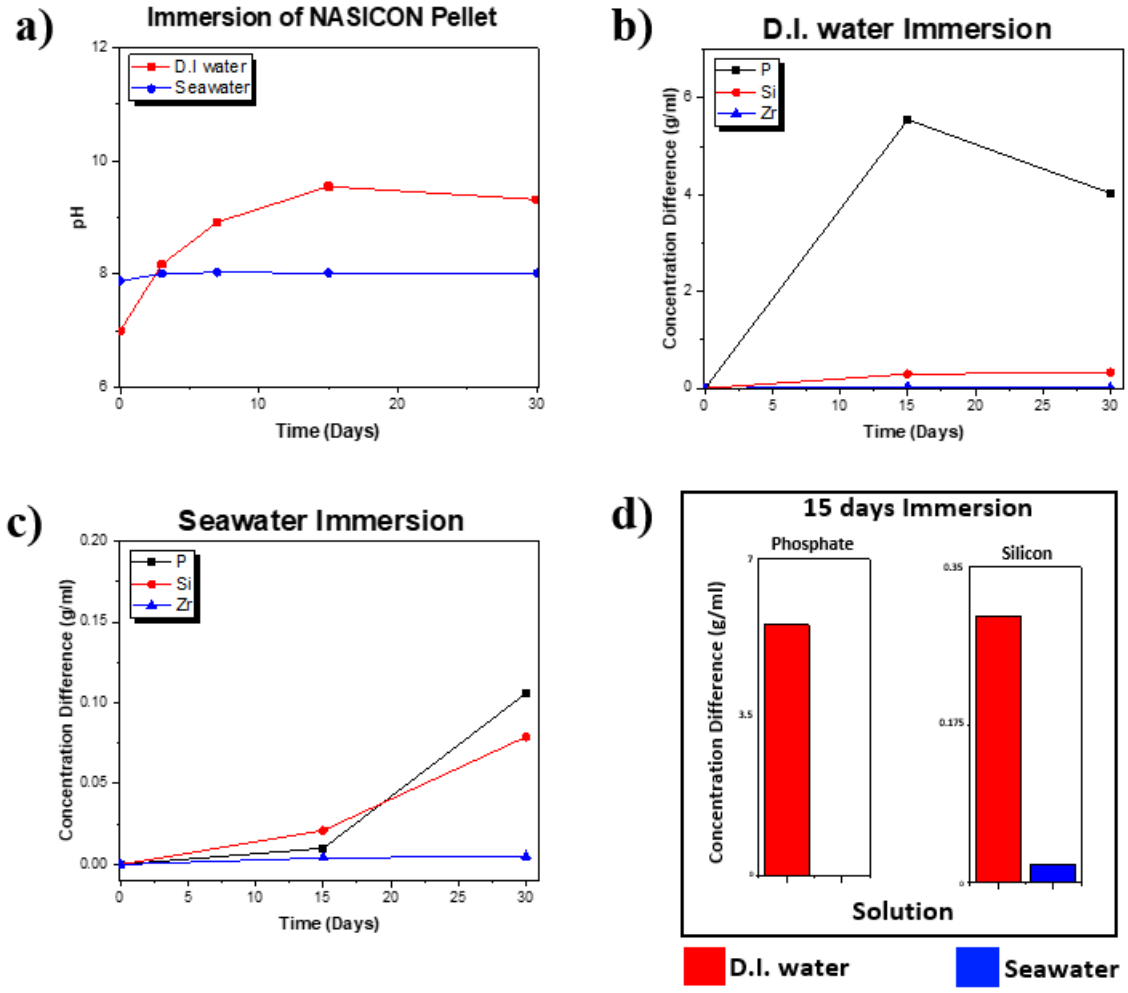

Figure 29. a) pH of NASICON immersion in D.I. water (blue) and Seawater (green), ICP result of Phosphate, Zirconium, and silicon in b) D.I. water and c) seawater, and comparison of the cations in D.I. water (red) and seawater (green) after 15 days of immersion

Seawater consist of natural salt ions and these ions might create difference secondary phase dissolution compare to D.I. water. To prove this hypothesis, NASICON powder is immersed in the salt solution at various NaCl concentration (Figure 30a). Notice that the powder was used to increase the speed of dissolution since the dissolution of the secondary phase is faster at bigger surface area. The immersion in various NaCl concentration shows that the slight addition of salt concentration may affect the saturation pH dramatically. Further addition of NaCl salt will affect the pH slightly. The saturated pH can be further decreased by the addition of different salt which exists in seawater (Figure 30b). Furthermore, the solubility of possible secondary-phase in NASICON (Na_2SiO_3 and Na_3PO_4) are checked and dissolved in D.I. water and seawater and the solubility of these compound was decreased dramatically (Figure 30c). Thus, the secondary phase dissolution happens less in seawater due to the existence of natural salt ions in seawater.

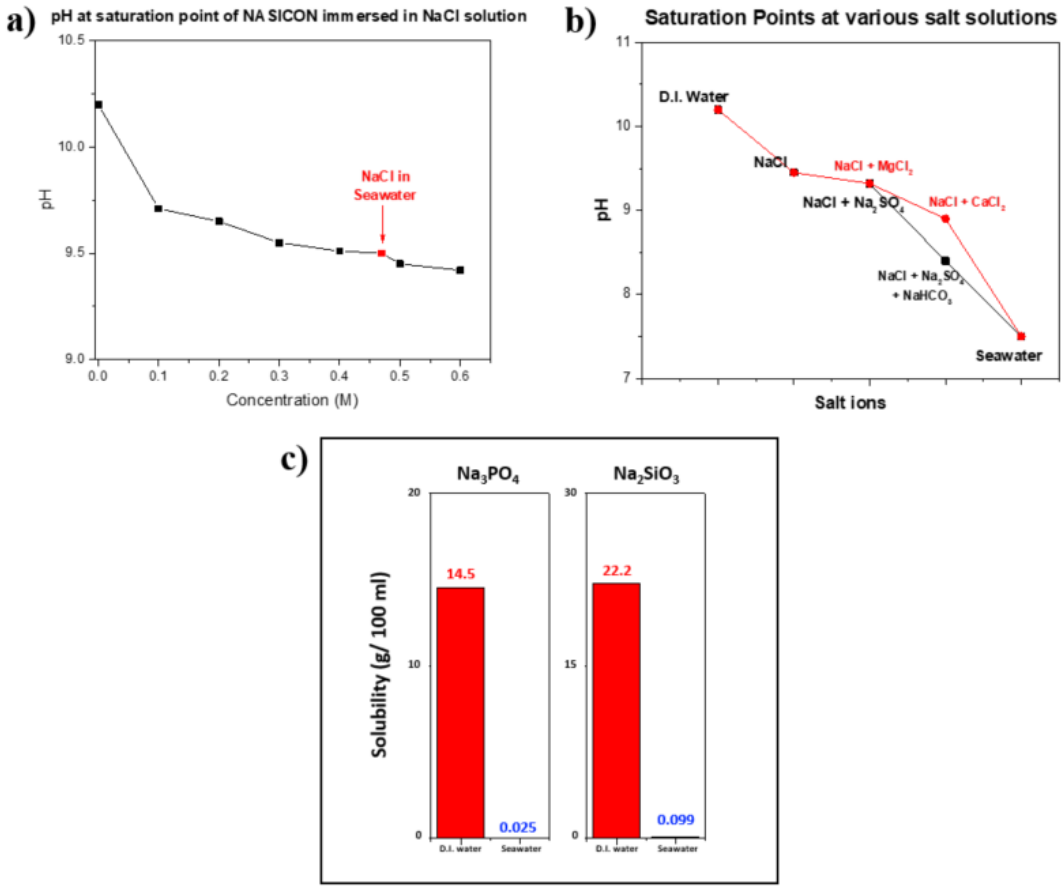

Figure 30. a) NASICON immersion in various concentration of NaCl, b) NASICON immersion in various salt which exists in seawater (the concentration of each salt is similar as the concentration available in seawater), and c) possible secondary phase solubility in D.I. water (red) and seawater (green)

The mechanical and electrochemical properties of NASICON is analyzed after 30 days immersion to show the effect of secondary phase dissolution in D.I. water and seawater toward NASICON property. The Ionic conductivity of immersed NASICON in D.I. water and seawater slightly decreases, but still considerably high around 10^{-4} S/cm (Figure 31a). This slight error is reasonable since the fabrication of NASICON pellet with exact properties is difficult. On the other hand, the mechanical strength weakens at longer immersion, especially in D.I. water, but seems more stable in seawater (Figure 31b). The slight decrease in properties might be due to the secondary phase dissolution, creating a hole and slightly decrease the properties. Although the reaction slightly affects the properties, however, NASICON is still usable for solid electrolyte application since the NASICON pellet doesn't show any sign of crack and the conductivity is still good enough to be applied in the battery.

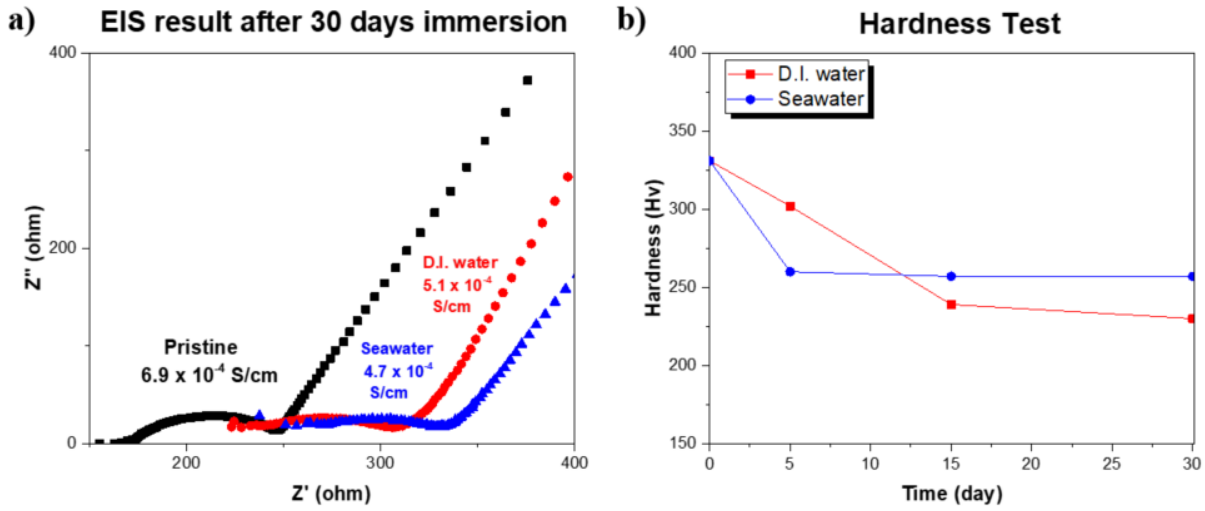

Figure 31. a) The EIS result of Pristine NASICON and NASICON after 30 days immersion in D.I. water and seawater, and b) Hardness test result of NASICON after the immersion in D.I. water and seawater

To summarize, the secondary phase dissolution happened in D.I. water and seawater regardless of the temperature and the mechanism is illustrated in Figure 32. This dissolution phenomenon couldn't be detected through pellet analysis because the number of secondary phases dissolved is a very tiny amount, thus the solution analysis becomes the primary analysis to understand the mechanism. Based on the previous result, the secondary phase dissolution peaked after 15 days and affect the pH of D.I. water. On the other hand, the pH of seawater seems not affected even after 1 month. The ICP result shows lesser dissolution in seawater compared to D.I. water. The lesser secondary phase dissolution happens in seawater due to the existence of natural salt ions in the seawater. The secondary phase affects the properties slightly, but the secondary-phase is not destructive. A longer period of immersion will be discussed in the next section.

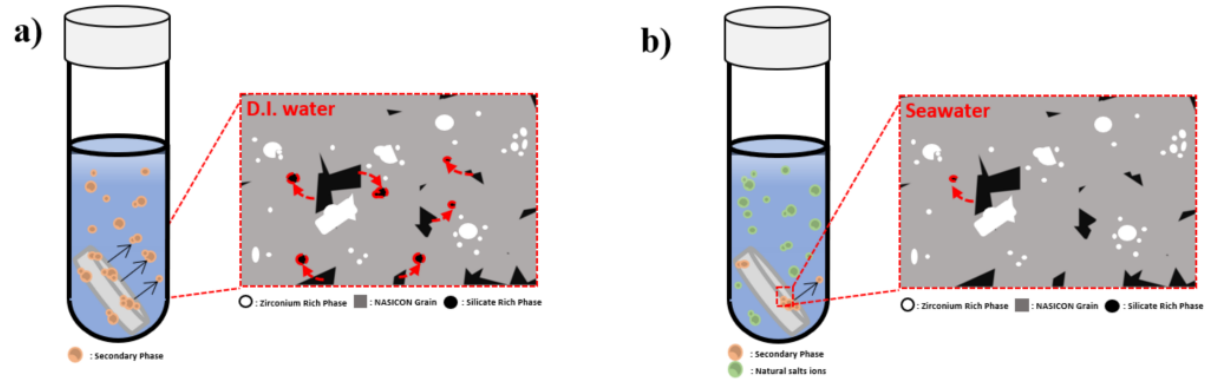

.

Figure 32. The illustration of secondary phase dissolution in a) D.I. water and b) seawater

3.3 Hydronium exchange reaction

Hydronium exchange reaction between Hydronium-ions from aqueous solution and Sodium-ions inside the NASICON is proven to happen at extreme condition such as high temperature or low pH solution (acidic condition). In this reaction, the Sodium inside NASICON is substituted with Hydronium-ions creating lower ionic conductivity and mechanical strength. [55] However, the stability of NASICON against room temperature in D.I. water and seawater are still unknown. To confirm this problem, the fabricated pristine NASICON will be immersed at a long period of time and analyzed. Figure 33 shows the XRD analysis of immersed NASICON in D.I. water and seawater after 30 days, 90 days, and 365 days. According to the previous report, Hydronium exchange reaction was only observed on three different regions (17.5° – 21.5°, 28.5° – 32.5°, and 32.5° – 36.5°) in XRD and these regions will be focused throughout this report. [55]

Based on Figure 33a, NASICON didn't show any new peak appearance after 30 days of immersion in D.I. water at room temperature. However, a tiny peak appeared at around 18.5° and 29.7° after 90 days immersion. The appearance was also followed by the decrement of the peak at 19.1° and 30.5°. Although Hydronium NASICON peal supposed to show up at around 35.4o, the peak wasn't observed since it's shorter compared to other Hydronium NASICON peak and will come out after severe detrimental by substitution. [55] A longer period (365 days), the new peak at 19.1° and 30.5° were slightly grown while the nearby corresponding pristine NASICON peak decreased. Furthermore, the peak split was observed in the first region at around 20°. These peak appearances will be analyzed further in the later section.

In case of seawater immersion (Figure 33b), the same pattern with D.I. water immersion observed on 30 days immersion, however, the difference can be seen at longer immersion. At 90 days 365 days immersion in seawater, there is no new peak observed at the first and second regions, especially on 18.5° and 29.7°, but the intensity at 19.1° was still decreased. The peak decrement became abrupt at 365 days immersion and almost every peak lost its sharpness, especially the peak at 30.1°. On the other hand, the XRD result didn't show any additional natural salt peaks in NASICON. Therefore, the salt was most likely sticking on the surface and can be easily washed.

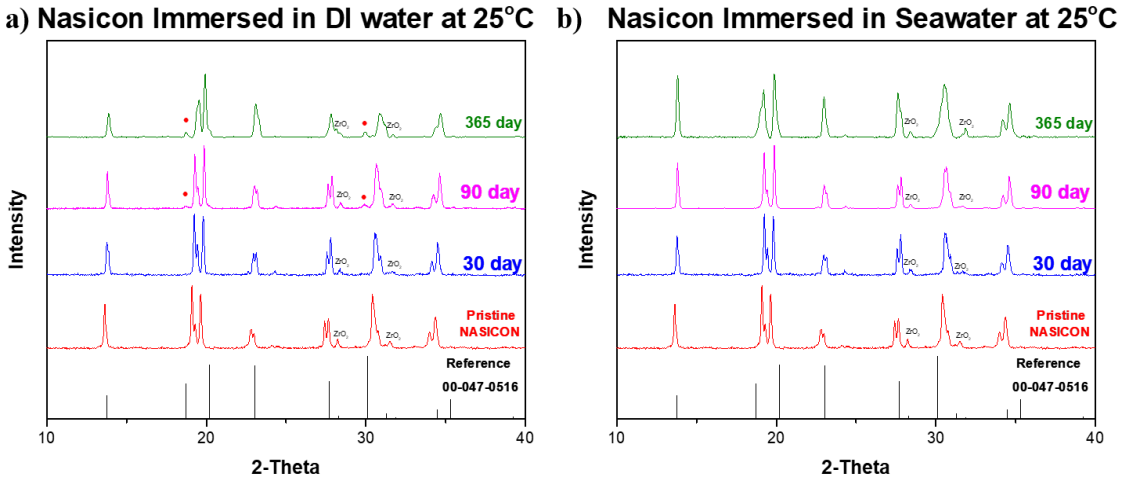

Figure 33. XRD comparison between reference NASICON, pristine NASICON, and NASICON immersed in a) D.I. water and b) seawater after 30 days, 90 days, and 365 days

Further analysis of X-ray diffraction is done in the first region (17.5° – 21.5°) since this region showed the most noticeable changes in both D.I. water and seawater immersion. Figure 34 summarized the peak change between pristine and 90 days immersion in D.I. water and seawater. There are two different change in XRD peaks that might correspond with two different reactions. Firstly, the intensity of NASICON peak change at 19.1° and 19.7° in both D.I. water and seawater immersion. Lastly, the appearance of a new peak at 18.5° and 20.1° at 365 days immersion, which only observed in D.I. water, but not seawater.

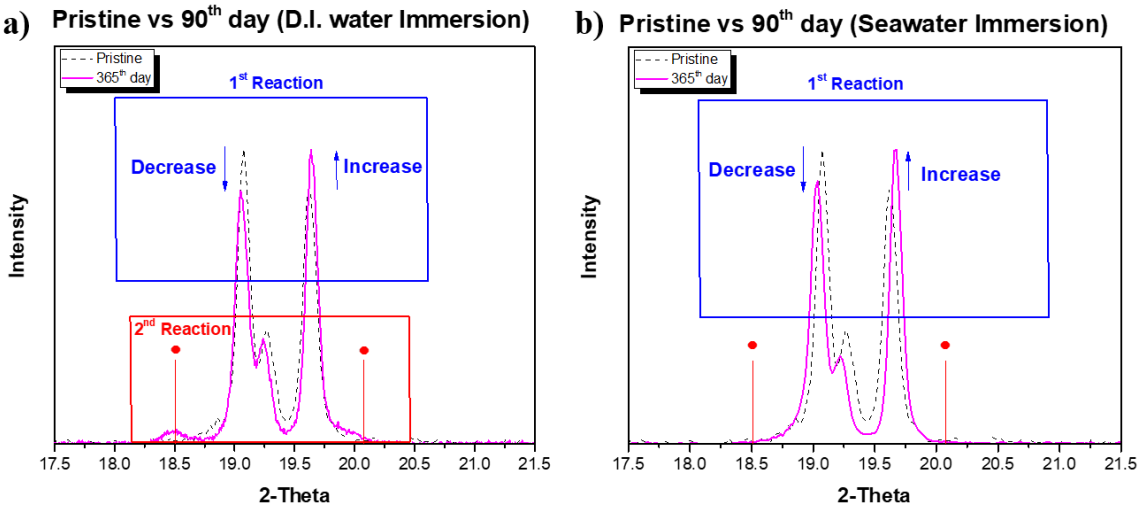

Figure 34. Further analysis of the first region (17.5°-21.5°) at 90 days immersion in a) D.I. water and b) seawater

3.3.1 Sodium diffusion out from NASICON

The intensity changed in NASICON was reported previously at NASICON immersion in seawater after 60 days (around 2 months). [29] This report is accurate and in fact, the intensity change happened much earlier during immersion in both D.I. water and seawater. Figure 35a shows the 30 days immersion in D.I. water and seawater and although the peak at 19.1° didn't decrease, however the other peak (at 19.7°) shows increment which decreases the ratio between these two peaks. The ratio between peak 1 (at 19.1°) and peak 2 (at 19.7°) is decreased as time goes on (Figure 35b). This intensity change might not be related to Hydronium NASICON since the peak can be reduced further without the appearance of a new peak (Figure 34 and Figure 35b). Therefore, this reaction might be independent to Hydronium-ions insertion.

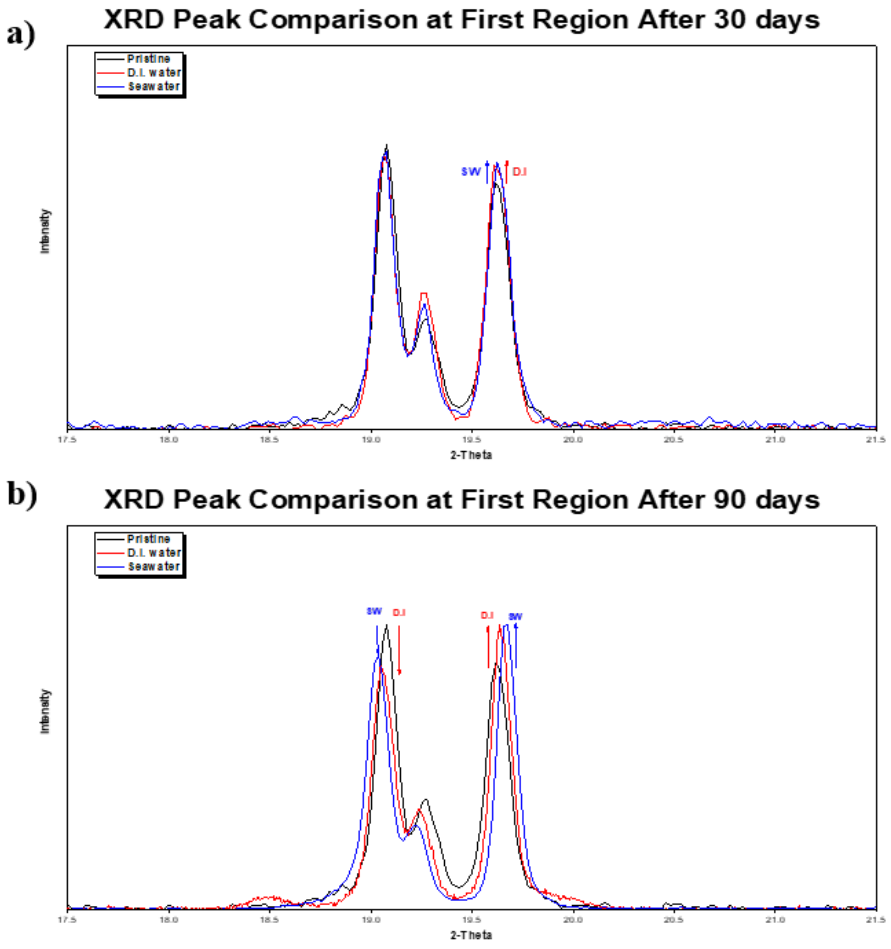

Figure 35. XRD peak comparison between pristine NASICON and immersed NASICON in D.I. water and seawater after a) 30 days and b) 90 days

To understand this region, further study of NASICON family ($Na_{1+x}Zr_2Si_xP_{3-x}O_{12}$, x= 0, 1.6, 2.0, and 2.25) was done by comparing the references as illustrated in Figure 36. There are three different patterns that are observed as the x decreased. Firstly, the ratio between peak 1 (19.1°) and peak 2 (19.7°) decreased. Secondly, the shifting of the peaks toward the higher angle in XRD. Lastly, a single peak observation instead of splitting at most of the peak around 10° - 40°. The first pattern perfectly described the changed in both D.I. water and seawater after immersion. The second pattern as observed after further immersion in D.I. water and seawater. Lastly, the last pattern which decreases the sharpness of each peak in both immersions. These changes are not related to Silicon and Phosphate modification inside the pristine NASICON. Silicon escape from the grain is impossible since the ICP result observed no increment after 15 days while the intensity started to change after 30 days of immersion. In addition, the Silicon escaped came from the secondary phase and not from the NASICON grain. The phosphate addition is theoretically impractical because D.I. water consists no ions, just pure H_2O. Thus, the most probable result is Sodium diffusion from grain to the solution. [39,40,67]

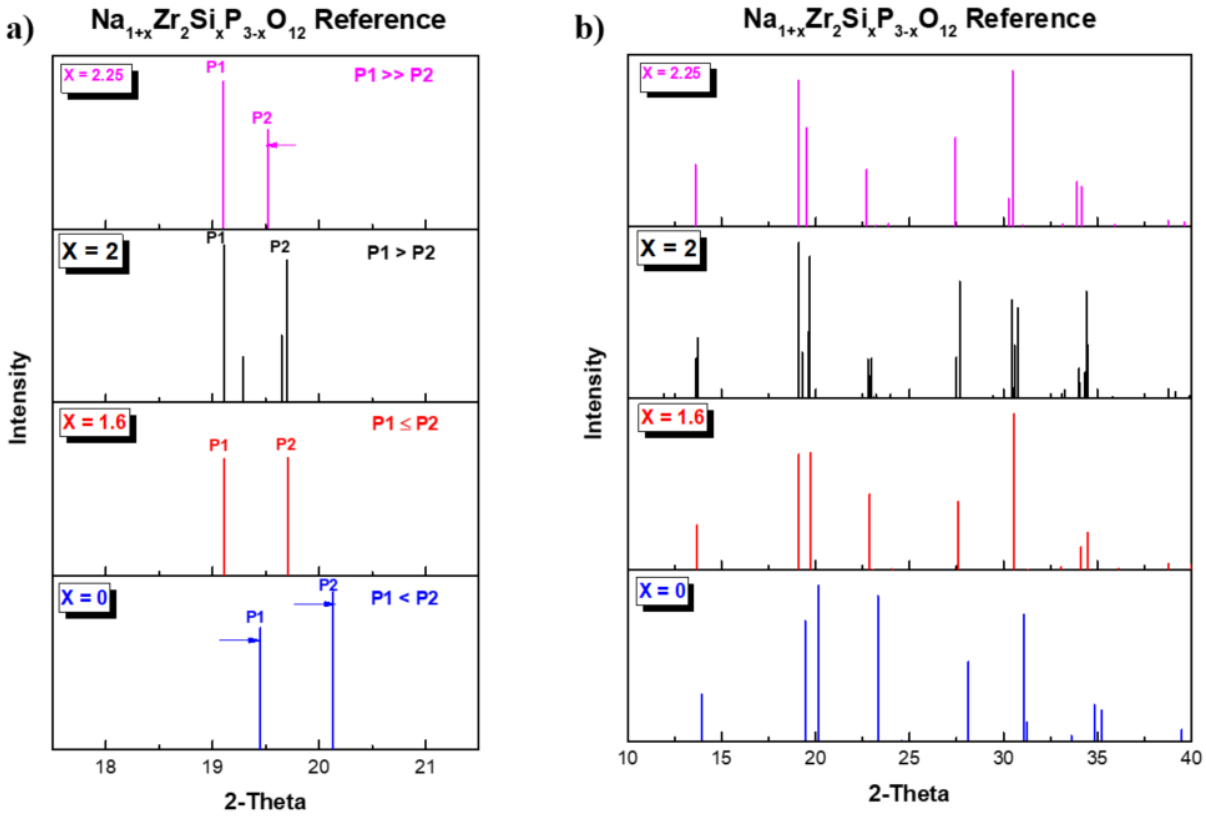

Figure 36. NASICON family reference comparison ($Na_{1+x}Zr_2Si_xP_{3-x}O_{12}$, x= 0, 1.6, 2.0, and 2.25) at a) first region (19.5° – 21.5°) and b) full range from 10° - 40° [39][40][67]

To proof that the Sodium diffused out from the NASICON grain, the Backscattered electron SEM-EDX of immersed NASICON in seawater and D.I. water is analyzed and shown in Figure 37. Based on the image (Figure 37a-b), both NASICON still maintained cubic shaped on the surface and there is hardly any difference between them. The EDX was taken at the grain NASICON of each SEM image and shows only sodium peaks decreased in both samples (Figure 37c). Thus, it's confirmed that the intensity ratio and broadness changes were due to Sodium diffusion out from NASICON to a solution. In addition, the EDX also confirmed that there is more Oxygen in the grain site of NASICON after 365 days immersion in D.I. water, which might be related to Hydronium-ions insertion. Thus, further analysis of the Hydronium-ion insertion will be discussed in the next section.

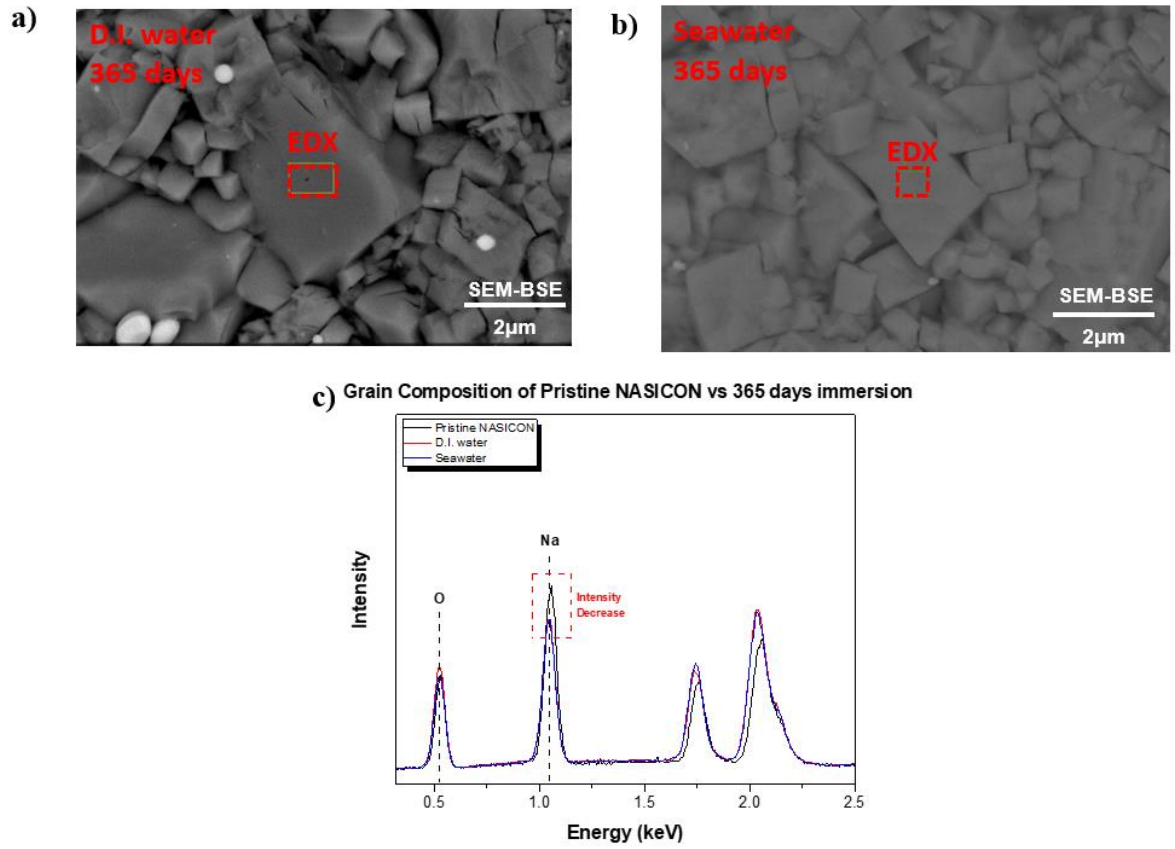

Figure 37. Surface BSE-SEM image of 365 days NASICON immersed in a) D.I. water and b) seawater with c) corresponding peak by EDX

3.3.2 Hydronium-ions insertion

The second reaction was corresponded to the peak appearance at 18.5° and 29.75° after 90 days immersion in D.I. water at room temperature, and peak split at 20.25° after 365 days immersion. These peak appearances are reported to have a similar pattern as hydronium NASICON peaks. However, the Hydronium NASICON reference has a composition of $(H_3O)_{2.5}Zr_2Si_{1.5}P_{1.5}O_{12,}$ which correspond to the fully exchanged NASICON at the formula of x = 1.5. This might be slightly inaccurate for comparison since the fabricated NASICON for experiment has a formula of $Na_3Zr_2Si_2PO_{12}$ (x = 2). Therefore, fabricating fully exchanged Hydronium NASICON with the experimental pristine NASICON will be beneficial since the fabricated compound is not only can accurately detect the Hydronium peaks but also can confirm the final product of fully exchanged Hydronium NASICON.

To fabricate Hydronium NASICON, the NASICON powder (x = 2.0) was refluxed with 0.5 M HCl for 2 hours. The solution is filtered and replaced with new 0.5 M HCl solution for 5 times. The finished product obtained and analyzed by using SEM (surface) and XRD. The structure of NASICON was compared by using XRD and the result shows almost similar peak as Hydronium NASICON reference (x = 1.5). The surface of Hydronium NASICON by SEM is a bit spherical on the sides and less rigid cubic compared to the NASICON (Figure 38a-b). The composition of NASICON is taken by EDX through SEM and EDX confirm the Sodium is fully exchanged since there is no Sodium detected and the abnormal Oxygen increment. In addition, Silicon, Zirconium, and Phosphate ions were still detected and weren't dissolved during the reaction due to the similar composition as pristine powder NASICON. Based on this information, the Hydronium exchange is possible to replace every sodium inside NASICON (x = 2), and the reaction follows the formula below. [62, 63]

$$\mathbf{Na_3Zr_2Si_2PO_{12} + 3\ H_3O^+ \rightarrow (H_3O)_3Zr_2Si_2PO_{12} + 3\ Na^+ \quad (10)}$$

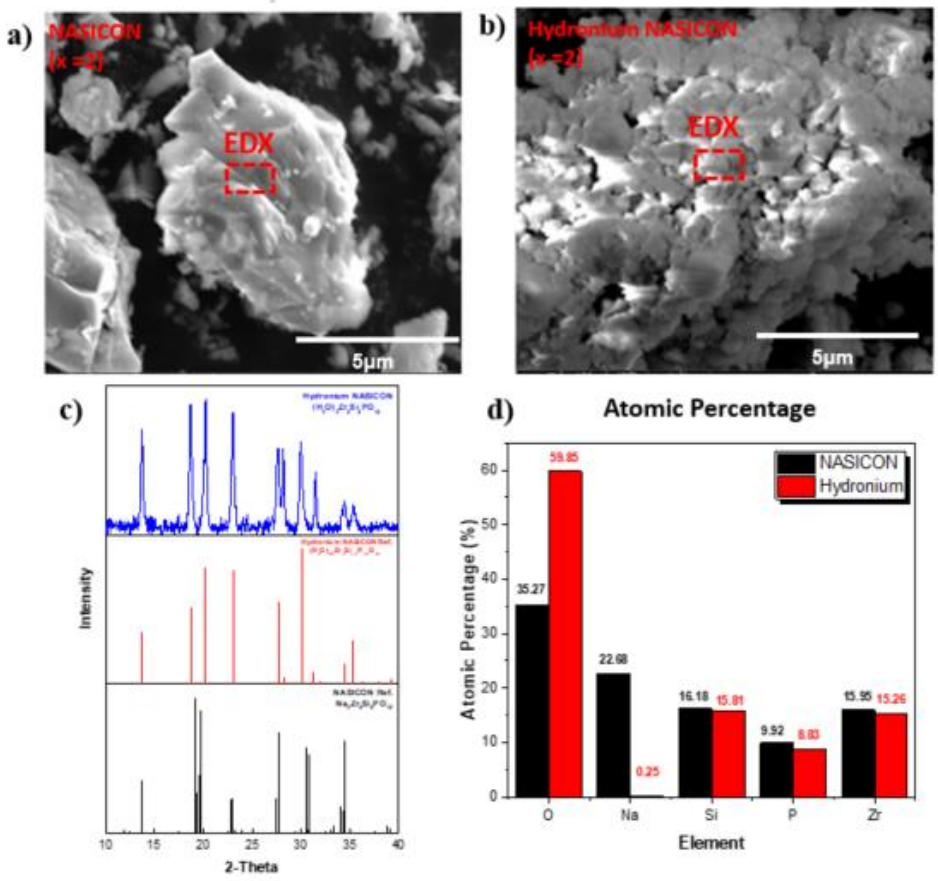

Figure 38. The SEM image of a) pristine powder NASICON and b) the powder of fully exchanged Hydronium NASICON. c) The XRD diffraction result of fully exchanged Hydronium NASICON (x = 2.0) and comparison with NASICON (x = 2) and Hydronium NASICON reference (x = 1.5) and the EDX comparison of previous SEM image

The fabricated Hydronium NASICON is compared with the immersed NASICON after 365 days in D.I. water since the Hydronium-ion peaks appearance was observed only in room temperature D.I. water (Figure 39). The Fully exchanged NASICON has a similar peak with the newly appeared peak at 18.5°, 20.25°, and 29.75°. In addition, the broader peak at the third region has a similar shape as Hydronium NASICON. However, the reaction is not yet severe, thus the short peak at around 33.4° couldn't be observed. To support the XRD result, other instrumental analyses such as TOF-SIMS and EELS were done.

The Hydronium-ions insertion to the NASICON is also supported by other instrumental analysis. Figure 40 shows the abnormal oxygen increment which comes from the Oxygen in the Hydronium-ions composition (H_3O^+). In addition, TOF-SIMS detects a tiny amount of hydronium ions on the thin surface of NASICON (Figure 40a). Although Hydronium-ions was detected in 90 days immersion in D.I. water, however, these ions couldn't be observed in seawater immersion. Another instrumental analysis is done by Electron Energy Loss Spectroscopy (EELS) after 180 days immersion and the disappearance peak at around 540 eV only in D.I. water was observed (Figure 40 b-d, the disappeared peak is marked with "*"). This disappearance happens nearby oxygen and might relate to Hydronium-ions insertion to NASICON lattice, creating disturbance in oxygen bonding of Zirconium octahedral and PO_4 or SiO_4 tetrahedral. Based on these observations, there are three things that can be summarized: 1. The peak appearance corresponds to the Hydronium-ions insertion, 2. The reaction did not happen in seawater immersion at room temperature (up to 365 days), 3. Only a tiny number of Hydronium-ions inserted since the hydronium peak is still dominating the XRD pattern.

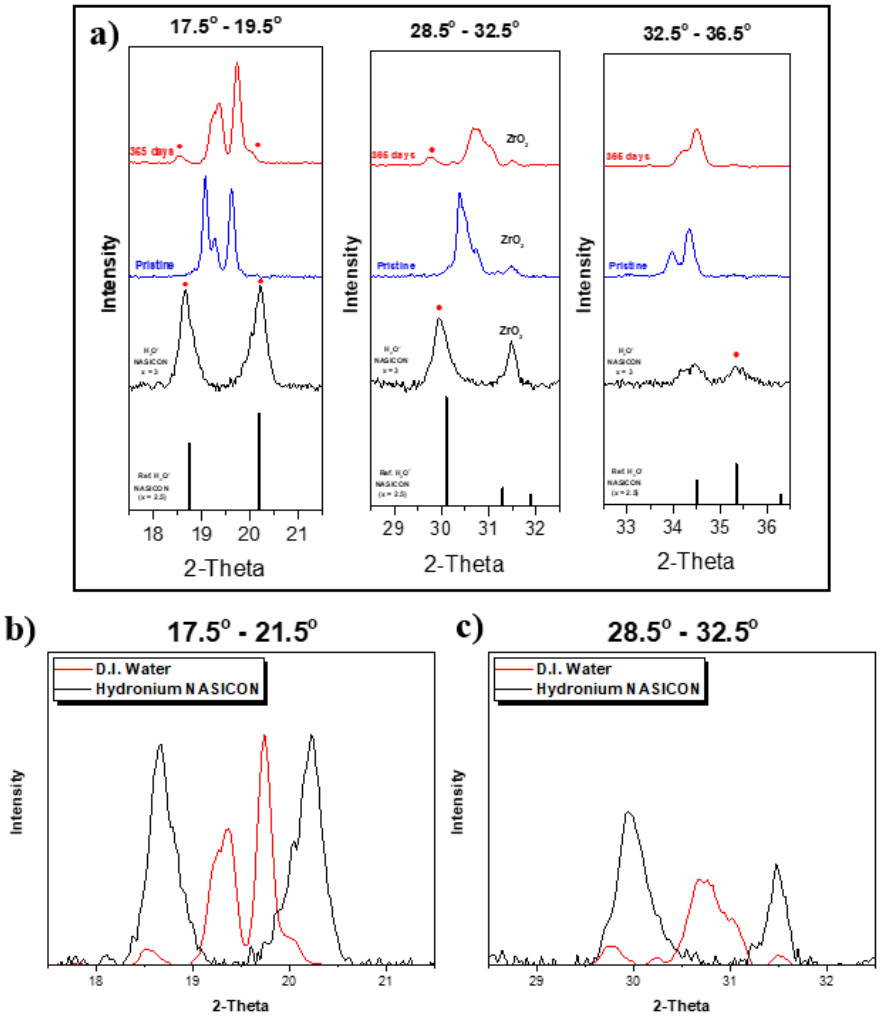

Figure 39. a) Hydronium NASICON (x = 2) comparison with NASICON immersed in D.I. water (365 days) at three important regions and further comparison between immersed NASICON and Hydronium NASICON at a) 17.5º - 21.5º and b) 28.5º – 32.5º

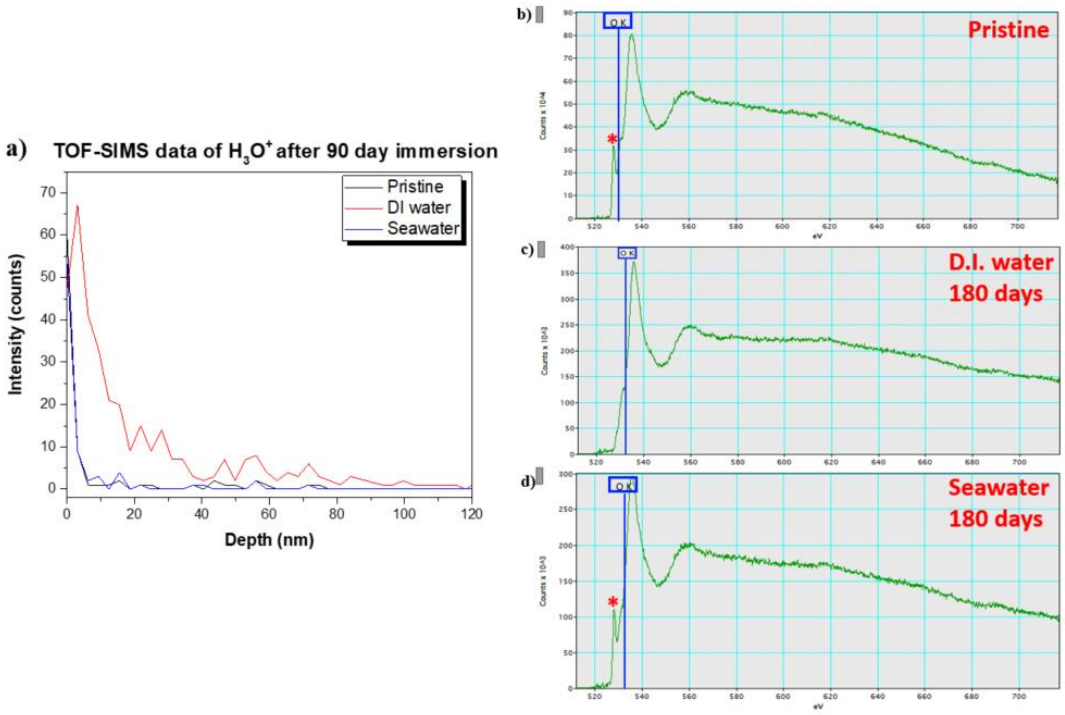

Figure 40. a) The Hydronium detection of pristine NASICON and 90-day immersed NASICON (D.I. water and Seawater), and b) EELS result of 180-day pristine and immersed NASICON

Based on the information above, the Hydronium-ions insertion is confirmed only in D.I. water. Although the Sodium kept diffusing out from NASICON to both D.I. water and seawater, however, the Hydronium-ions couldn't be inserted into the empty crystal lattice. This phenomenon can be explained through the doping energy barrier formula shown below: [65][66]

$$\Delta E_{H_3O^+-NAS} = E_{H_3O^+} - E_{NAS} + u_{Na^+} - u_{H_3O^+} \quad (11)$$

$$u_{H_3O^+}(T,p) = u_{ref}(T,p) + k_B T\, u \ln\left(\frac{p}{p_0}\right) \quad (12)$$

$\Delta E_{H_3O^+-NAS}$ = *Energy barrier difference,* $E_{H_3O^+}$ = *Energy barrier of Hydronium NASICON*

E_{NAS} = *Energy barrier of NASICON* u_{Na^+} = *Chemical Potential of Sodium-ions in solution*

$u_{H_3O^+}$ = *Chemical potential of Hydronium-ions* T = *Temperature*

p = *pressure* k_B = *Boltzmann constant*

If the ΔE_{doped} is negative (below 0), then the Hydronium-ions insertion happen spontaneously, however, the reaction won't happen if the energy difference is positive. This variable is affected by the chemical potential of Sodium-ions in the solution, chemical potential of Hydronium-ions, and temperature. As the concentration of Sodium-ions increased in solution, the chemical potential increase which result in the increase ΔE_{doped} of Hydronium-ions insertion. The chemical potential of Hydronium-ions also affected by pH and it's less reactive at high pH (low H_3O^+ chemical potential) and active at the acid condition. This phenomenon is already reported by Jae-il Jung et al and taken as adan vantage for Hydronium NASICON fabrication. [59] Lastly, the temperature affects the chemical potential of the solution since temperature increases the H_3O^+ chemical potential. Based on this equivalence, the Hydronium-Ions insertion is predicted to happen less or even inactive at room temperature seawater. Firstly, the seawater has higher pH than D.I. water, thus the chemical potential is predicted to be lower. Lastly, the chemical potential of Sodium ions in seawater is higher due to the existence of Sodium-ions. However, the stability of NASICON at high temperature is not known and the effect of another ions except Sodium.

To understand the effect of temperature toward the Hydronium exchange reaction, the pristine NASICON was immersed at 80°C in D.I. water and seawater (Figure 41). At high-temperature immersion, the hydronium NASICON peak appears at both NASICON immersed in D.I. water and seawater even after 12 hours, and the appearance is at the exact location as the immersed NASICON at room temperature in D.I. water. The temperature affects the NASICON stability dramatically since the reaction at 80°C for 12 hours has a similar result as 90 days immersion in D.I. water. At longer period high-temperature immersion, the Hydronium NASICON peak grows up as the pristine NASICON peak falls. Although the Hydronium-ions insertion also observed in seawater at high temperature, however, the growth of hydronium peaks was much slower than D.I. water immersion. At 60°C immersion for 10 days (Figure 42), the result shows that the reaction became slower, and this reaction is almost similar as the 365 days immersion in D.I. water due to the appearance of the peak at 20.1° and no appearance of the peak at 35.5°. Thus, the temperature accelerates the Hydronium-ions insertion rapidly. Although the reaction shows in the seawater immersion, however, it tends to be slower than D.I. water and wasn't observed at room temperature.

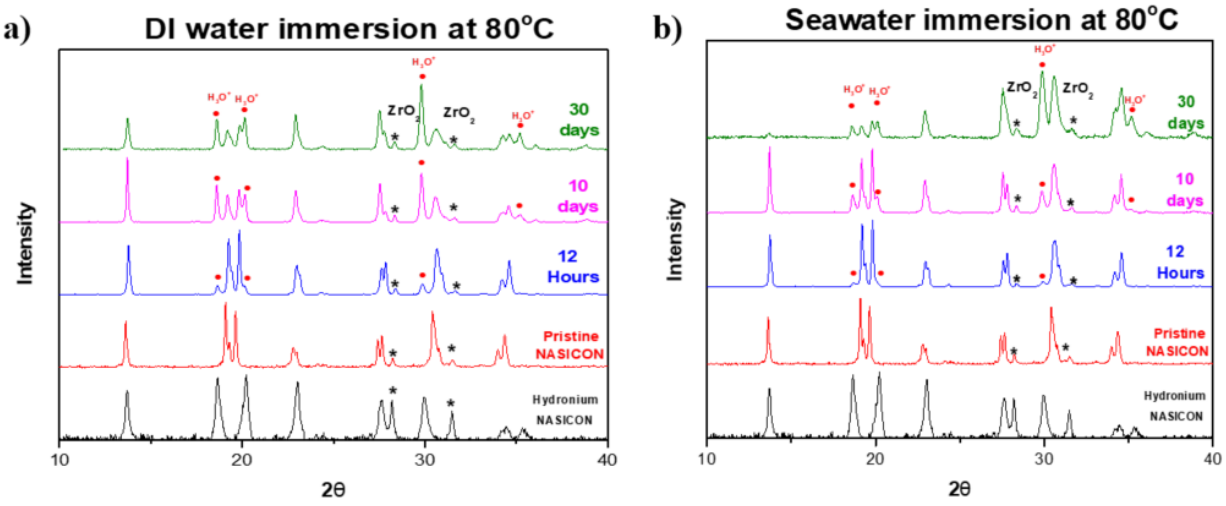

Figure 41. NASICON immersion at high temperature (80ºC) after 12 hours, 10 days, and 30 days in a) D.I. water and b) Seawater

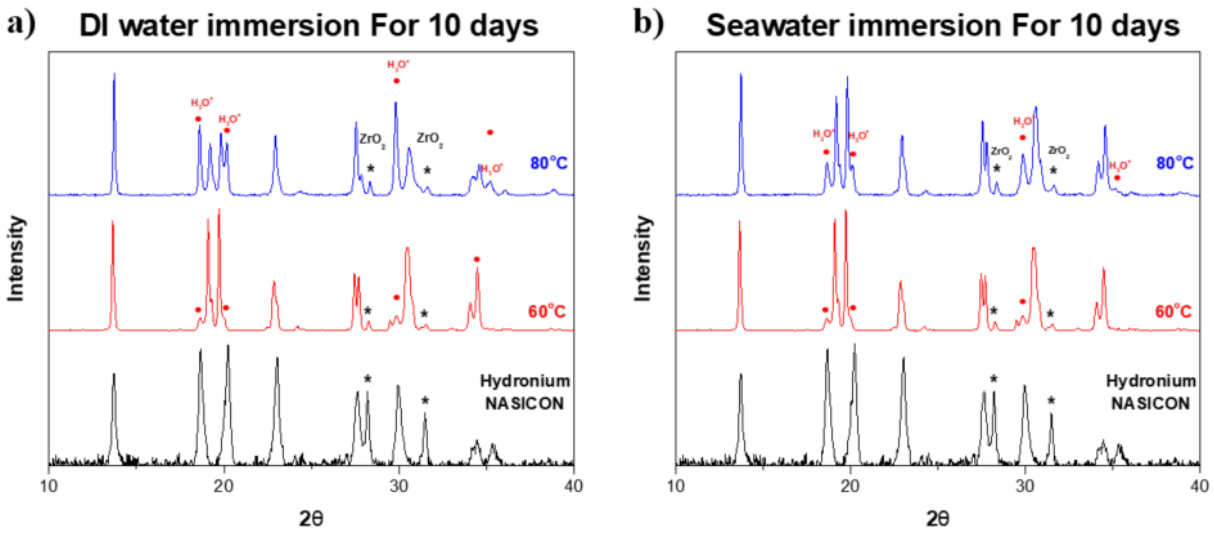

Figure 42. NASICON immersion after 10 days at 60ºC and 80ºC in a) D.I. water and b) Seawater

According to the high-temperature immersion, the result shows that Hydronium-ions insertion is slower in seawater than D.I. water. This phenomenon might be affected by the natural salt ions that exist in seawater as suggested by equation 8. To confirm the effect of natural salt ions inside seawater, the pristine NASICON was immersed in 0.1 M NaCl for at high temperature for 30 days (Figure 43a). Based on the XRD result, the peak appears lower compared to the D.I. water immersion, which means it's less reactive. This result corresponds to the proposed equation (11). The image of the NASICON pellet is taken after 30 days immersion and NASICON immersed in D.I. water broke into pieces (Figure 43b). This is possible since Hydronium-ions has bigger volume than Sodium-ions, thus create a crack in structure and breaking the pellet at excess insertion. [55] Surprisingly, the addition of 0.1 M NaCl to the solution can prevent NASICON from breaking/ However, the NASICON become very fragile compared to the pristine NASICON. The reference intensity ratio (RIR) at 29.7° was taken as a comparison since the exchanged is more noticeable compared to the peak at 19.5° (with RIR at 66.5% in fully exchanged Hydronium NASICON). As the ions added to the solution, the RIR shows lesser value, which also means a lower reaction rate. Thus, the ions affect the stability of NASICON in seawater indirectly.

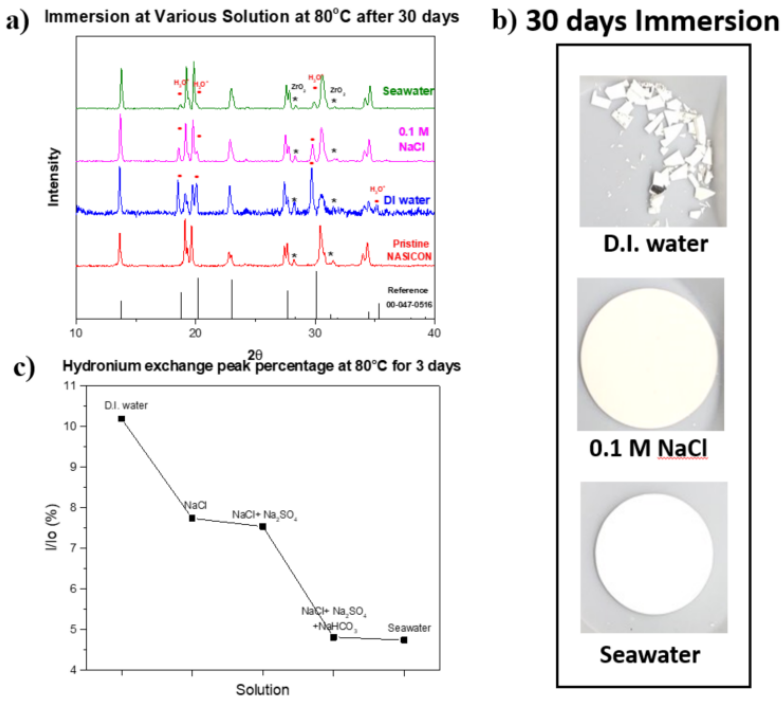

Figure 43. a) XRD result of NASICON immersion in D.I. water, 0.1 M NaCl at 80°C, and Seawater for 30 days, b) pellet after 30 days immersion at 80°C, and the reference intensity ratio (RIR) at peak 29.7° of NASICON immersed at the different salt solutions (concentration based on the seawater) at 80°C

The electrochemical properties of NASICON immersion at room temperature is analyzed by using electrochemical impedance (Figure 44). In the case of seawater, the ionic conductivity slightly decreases to 3 x 10^{-4} S/cm after 180 days immersion. The slight decrease was most likely due to Sodium diffusion out from NASICON, thus lowering the mobile ions inside NASICON. However, the conductivity of NASICON was decreased dramatically to 9 x 10^{-6} S.cm after 90 days immersion in D.I. water only. The ionic conductivity decrement might be due to Hydronium-ions insertion since the conductivity fouling happens at the same time as Hydronium NASICON peak appearance in XRD. In addition, the TOF-SIMS detects Hydronium-ions only on the surface of NASICON suggesting that the Hydronium insertion couldn't penetrate deeply to NASICON. Thus, it's most likely that Hydronium NASICON hinders the conductivity only in the surface and the NASICON can be returned to pristine once the surface is removed. To prove this hypothesis, the surfaces of immersed NASICON was polished at around 0.1 mm and the EIS was taken (Figure 45). The NASICON ionic conductivity of polished sample return to the pristine and the XRD result shows no hydronium NASICON peak.

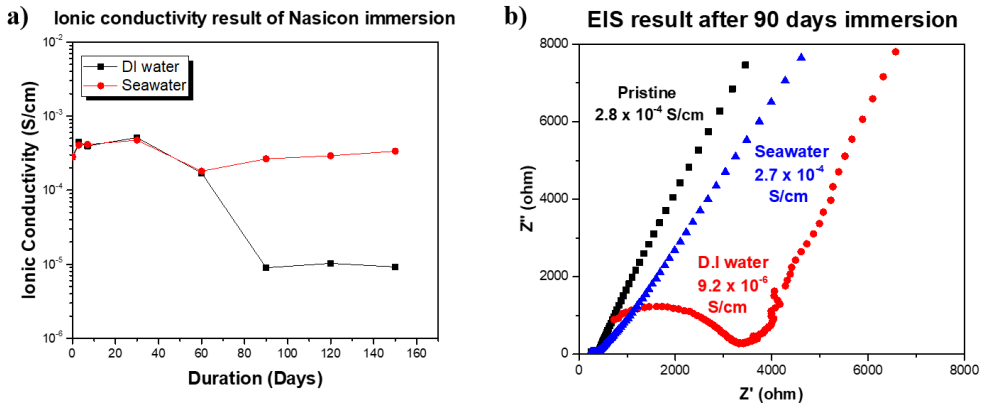

Figure 44. a) Ionic conductivity NASICON immersed in D.I. water and seawater after a certain time (up to 180 days) and b) EIS result after 90 days immersion

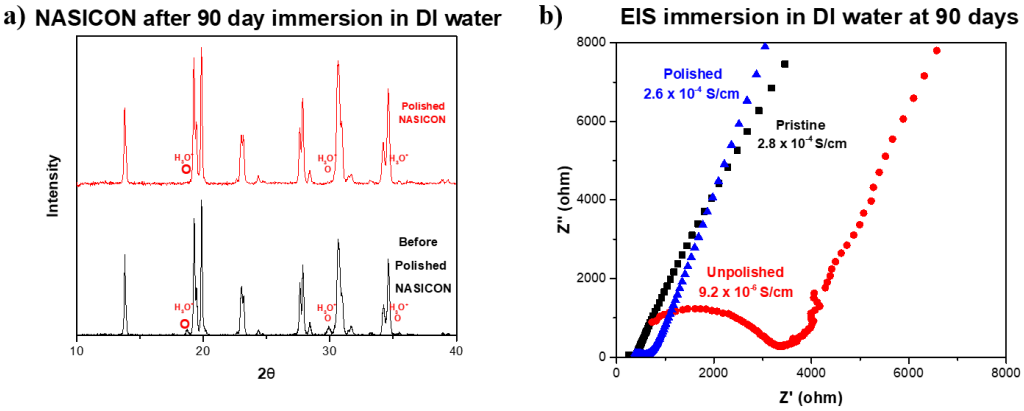

Figure 45. The a) XRD and b) EIS result of 90-day immersed NASICON before and after polished

To summarize, there are two different steps of Hydronium exchange reaction between NASICON and aqueous solution. Firstly, the Sodium diffused out from the NASICON and can be observed by the shifting and intensity change in XRD peaks. The reaction happens in any condition and slightly alter the conductivity. If the doped energy support, then the Hydronium-ions will be inserted into empty space from the Sodium escape. The Hydronium-ions insertion is destructive and possible to break NASICON if the insertion happens excessively. This reaction can be detected by XRD, TOF-SIMS, and EELS. The insertion is affected by few variables such as ions (especially Sodium-ions), pH, and temperature. These reactions are illustrated in Figure 46 below.

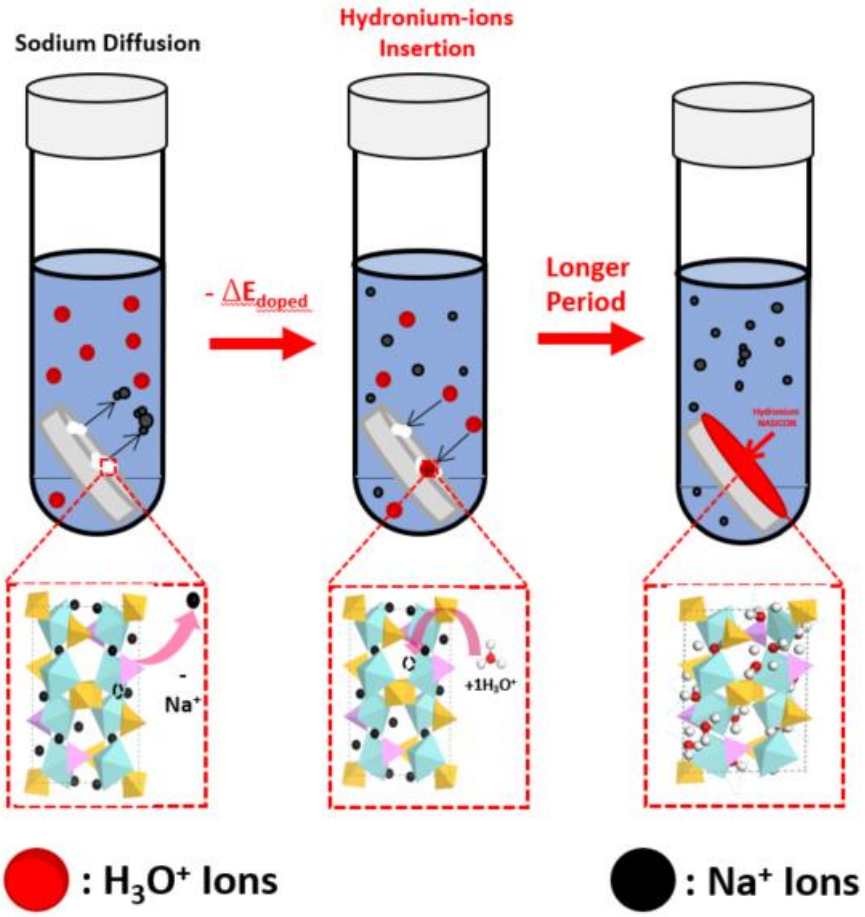

Figure 46. Illustration of Sodium diffusion and Hydronium-ions insertions in NASICON immersion at any solution

4. Conclusion

Based on this report, the NASICON reaction with D.I. water and seawater can be divided into three different mechanisms:

1. Firstly, Secondary phase dissolution happens as the NASICON in-contact with an aqueous solution. This reaction can be analyzed through the solution analysis. The immersion in NASICON shows more stable than in D.I. water due to the existence of natural salt ions, hindering the secondary phase dissolution. This reaction affects slightly to the mechanical and electrochemical properties.
2. Secondly, the Sodium diffusion out from NASICON grain into the solution is observed after the secondary phase dissolution through the change in intensity peak and peak-shifting in X-ray diffraction of immersed NASICON in both D.I. water and seawater at room temperature. The Sodium diffusion slightly lowers the electrochemical properties, but NASICON is still usable as a solid electrolyte.
3. Lastly, Hydronium-ions insertion arises if only the energy barrier requirement is fulfilled. This energy barrier is directly depending on pH, temperature, Sodium-ions concentration, and indirectly correlated with other natural salt ions. This reaction created a new peak on X-ray diffraction and may break NASICON if excess insertion happened (especially at high temperature). The electrochemical properties fall greatly to 10^{-6} S/cm due to hydronium NASICON coated on top of thin surface NASICON. This reaction might create failure to the seawater battery due to low ionic conductivity and possibly breaking NASICON at excess insertion.

The immersion in D.I. water at room temperature undergoes these three mechanisms after 90 days. On the other hand, there is no proof on Hydronium-ions insertion in the seawater at room temperature even after 365 days. The conductivity greatly changes in D.I. water while still maintain a reasonable conductivity in seawater after 180 days immersion. In conclusion, the immersion in seawater at room temperature is more stable than the immersion in D.I. water.

5. Reference

1. Luo, X., Wang, J., Dooner, M., & Clarke, J. (2015). Overview of current development in electrical energy storage technologies and the application potential in power system operation. Applied Energy, 137, 511-536. doi:10.1016/j.apenergy.2014.09.081
2. International Energy Agency. (2014,) Key World Energy Statistics 2014. (2014). Retrieved November 29, 2018, from <https://www.iea.org/>
3. Jebli, M. B., Youssef, S. B., & Ozturk, I. (2016). Testing environmental Kuznets curve hypothesis: The role of renewable and non-renewable energy consumption and trade in OECD countries. Ecological Indicators, 60, 824-831. doi:10.1016/j.ecolind.2015.08.031
4. Höök, M., & Tang, X. (2013). Depletion of fossil fuels and anthropogenic climate change—A review. Energy Policy, 52, 797-809. doi:10.1016/j.enpol.2012.10.046
5. Hughes, L. (2000). Biological consequences of global warming: Is the signal already apparent? Trends in Ecology & Evolution, 15(2), 56-61. doi:10.1016/s0169-5347(99)01764-4A
6. Jacobson, S., & Johnson, A. (2001). The diffusion of renewable energy technology: An analytical framework and key issues for research. Fuel and Energy Abstracts, 42(1), 46. doi:10.1016/s0140-6701(01)80501-4
7. Yang, Z., Zhang, J., Kintner-Meyer, M. C., Lu, X., Choi, D., Lemmon, J. P., & Liu, J. (2011). Electrochemical Energy Storage for Green Grid. Chemical Reviews, 111(5), 3577-3613. doi:10.1021/cr100290v
8. Dunn, B., Kamath, H., & Tarascon, J. (2011). Electrical Energy Storage for the Grid: A Battery of Choices. Science, 334(6058), 928-935. doi:10.1126/science.1212741
9. Nitta, N., Wu, F., Lee, J. T., & Yushin, G. (2015). Li-ion battery materials: Present and future. Materials Today, 18(5), 252-264. doi:10.1016/j.mattod.2014.10.040
10. Ibrahim, H., Ilinca, A., & Perron, J. (2008). Energy storage systems—Characteristics and comparisons. Renewable and Sustainable Energy Reviews, 12(5), 1221-1250. doi:10.1016/j.rser.2007.01.023
11. Tarascon, J. (2010). Is lithium the new gold? Nature Chemistry, 2(6), 510-510. doi:10.1038/nchem.680
12. Yabuuchi, N., Kubota, K., Dahbi, M., & Komaba, S. (2014). Research Development on Sodium-Ion Batteries. Chemical Reviews, 114(23), 11636-11682. doi:10.1021/cr500192f
13. Palomares, V., Serras, P., Villaluenga, I., Hueso, K. B., Carretero-González, J., & Rojo, T. (2012). Na-ion batteries, recent advances and present challenges to become low cost energy storage systems. Energy & Environmental Science, 5(3), 5884. doi:10.1039/c2ee02781j

14. Chayambuka, K., Mulder, G., Danilov, D. L., & Notten, P. H. (2018). Sodium-Ion Battery Materials and Electrochemical Properties Reviewed. Advanced Energy Materials, 8(16), 1800079. doi:10.1002/aenm.201800079
15. Kim, Y., Ha, K., Oh, S. M., & Lee, K. T. (2014). High-Capacity Anode Materials for Sodium-Ion Batteries. Chemistry - A European Journal, 20(38), 11980-11992. doi:10.1002/chem.201402511
16. Wen, Z., Hu, Y., Wu, X., Han, J., & Gu, Z. (2012). Main Challenges for High Performance NAS Battery: Materials and Interfaces. Advanced Functional Materials, 23(8), 1005-1018. doi:10.1002/adfm.201200473
17. Lu, X., Lemmon, J. P., Sprenkle, V., & Yang, Z. (2010). Sodium-beta alumina batteries: Status and challenges. Jom, 62(9), 31-36. doi:10.1007/s11837-010-0132-5
18. Mark, J. (1992). Environmental health, and safety issues of sodium-sulfur batteries for electric and hybrid vehicles. Golden, Col.: National Renewable Energy Laboratory.
19. Sudworth, J. L., Barrow, P., Dong, W., Dunn, B., Farrington, G. C., & Thomas, J. O. (2000). Toward Commercialization of the Beta-Alumina Family of Ionic Conductors. MRS Bulletin, 25(03), 22-26. doi:10.1557/mrs2000.14
20. Park, S., Senthilkumar, B., Kim, K., Hwang, S. M., & Kim, Y. (2016). Saltwater as the energy source for low-cost, safe rechargeable batteries. Journal of Materials Chemistry A, 4(19), 7207-7213. doi:10.1039/c6ta01274d
21. Sangmin, P. (2016). Designing a new battery system using NaCl aqueous solution as cathode (master's thesis, UNIST). Graduate School of UNIST.
22. Kim, J., Lee, E., Kim, H., Johnson, C., Cho, J., & Kim, Y. (2015). Inside Cover: Rechargeable Seawater Battery and Its Electrochemical Mechanism (ChemElectroChem 3/2015). ChemElectroChem, 2(3), 294-294. doi:10.1002/celc.201590010
23. Han, J., Hwang, S. M., Go, W., Senthilkumar, S., Jeon, D., & Kim, Y. (2018). Development of coin-type cell and engineering of its compartments for rechargeable seawater batteries. Journal of Power Sources, 374, 24-30. doi:10.1016/j.jpowsour.2017.11.022
24. Kim, J., Mueller, F., Kim, H., Bresser, D., Park, J., Lim, D., . . . Kim, Y. (2014). Rechargeable-hybrid-seawater fuel cell. NPG Asia Materials, 6(11). doi:10.1038/am.2014.106
25. Hwang, S. M., Kim, J., Kim, Y., & Kim, Y. (2016). Na-ion storage performance of amorphous Sb2S3nanoparticles: Anode for Na-ion batteries and seawater flow batteries. J. Mater. Chem. A, 4(46), 17946-17951. doi:10.1039/c6ta07838a

26. Kim, Y., Kim, J., Vaalma, C., Bae, G. H., Kim, G., Passerini, S., & Kim, Y. (2018). Optimized hard carbon derived from starch for rechargeable seawater batteries. Carbon, 129, 564-571. doi:10.1016/j.carbon.2017.12.059
27. Kim, Y., Hwang, S. M., Yu, H., & Kim, Y. (2018). High energy density rechargeable metal-free seawater batteries: A phosphorus/carbon composite as a promising anode material. Journal of Materials Chemistry A, 6(7), 3046-3054. doi:10.1039/c7ta10668h
28. Kim, H., Park, J., Sahgong, S. H., Park, S., Kim, J., & Kim, Y. (2014). Metal-free hybrid seawater fuel cell with an ether-based electrolyte. J. Mater. Chem. A, 2(46), 19584-19588. doi:10.1039/c4ta04937c
29. Kim, Y., Kim, H., Park, S., Seo, I., & Kim, Y. (2016). Na ion- Conducting Ceramic as Solid Electrolyte for Rechargeable Seawater Batteries. Electrochimica Acta, 191, 1-7. doi:10.1016/j.electacta.2016.01.054
30. Zheng, F., Kotobuki, M., Song, S., Lai, M. O., & Lu, L. (2018). Review on solid electrolytes for all-solid-state lithium-ion batteries. Journal of Power Sources, 389, 198-213. doi:10.1016/j.jpowsour.2018.04.022
31. Rankin, G. A., & Merwin, H. E. (1916). THE TERNARY SYSTEM CaO-Al2O3-MgO. Journal of the American Chemical Society, 38(3), 568-588. doi:10.1021/ja02260a006
32. Kummer, J. (1972). β-Alumina electrolytes. Progress in Solid State Chemistry, 7, 141-175. doi:10.1016/0079-6786(72)90007-6
33. Rice, M., & Roth, W. (1972). Ionic transport in super ionic conductors: A theoretical model. Journal of Solid State Chemistry, 4(2), 294-310. doi:10.1016/0022-4596(72)90121-1
34. Sudworth, J. L., & Tilley, A. R. (1986). The sodium sulfur battery. London: Chapman & Hall.
35. Beckers, J. (2000). Ionic conduction in Na -β-alumina studied by molecular dynamics simulation. Solid State Ionics, 133(3-4), 217-231. doi:10.1016/s0167-2738(00)00685-8
36. Wang, B., & Cormack, A. N. (2014). Molecular dynamics simulations of Mg-doped beta″-alumina with potential models fitted for accurate structural response to thermal vibrations. Solid State Ionics, 263, 9-14. doi:10.1016/j.ssi.2014.04.018
37. Lu, X., Xia, G., Lemmon, J. P., & Yang, Z. (2010). Advanced materials for sodium-beta alumina batteries: Status, challenges and perspectives. Journal of Power Sources, 195(9), 2431-2442. doi:10.1016/j.jpowsour.2009.11.120
38. Hagman, L., Kierkegaard, P., Karvonen, P., Virtanen, A. I., & Paasivirta, J. (1968). The Crystal Structure of NaM2IV(PO4)3; MeIV = Ge, Ti, Zr. Acta Chemica Scandinavica, 22, 1822-1832. doi:10.3891/acta.chem.scand.22-1822

39. Hong, H. (1976). Crystal structures and crystal chemistry in the system Na1 xZr2SixP3−xO12. Materials Research Bulletin, 11(2), 173-182. doi:10.1016/0025-5408(76)90073-8
40. Boilot, J., Collin, G., & Colomban, P. (1988). Relation structure-fast ion conduction in the NASICON solid solution. Journal of Solid State Chemistry, 73(1), 160-171. doi:10.1016/0022-4596(88)90065-5
41. Alpen, U. V., Bell, M., & Wichelhaus, W. (1979). Phase transition in nasicon (Na3Zr2Si2PO12). Materials Research Bulletin, 14(10), 1317-1322. doi:10.1016/0025-5408(79)90010-2
42. Goodenough, J., Hong, H., & Kafalas, J. (1976). Fast Na -ion transport in skeleton structures. Materials Research Bulletin, 11(2), 203-220. doi:10.1016/0025-5408(76)90077-5
43. Ignaszak, A., Pasierb, P., Gajerski, R., & Komornicki, S. (2005). Synthesis and properties of Nasicon-type materials. Thermochimica Acta, 426(1-2), 7-14. doi:10.1016/j.tca.2004.07.002
44. Park, H., Jung, K., Nezafati, M., Kim, C., & Kang, B. (2016). Sodium Ion Diffusion in Nasicon (Na3Zr2Si2PO12) Solid Electrolytes: Effects of Excess Sodium. ACS Applied Materials & Interfaces, 8(41), 27814-27824. doi:10.1021/acsami.6b09992
45. Boilot, J., Collin, G., & Colomban, P. (1987). Crystal structure of the true nasicon: Na3Zr2Si2PO12. Materials Research Bulletin, 22(5), 669-676. doi:10.1016/0025-5408(87)90116-4
46. Mazza, D. (2001). Modeling Ionic Conductivity in Nasicon Structures. Journal of Solid State Chemistry, 156(1), 154-160. doi:10.1006/jssc.2000.8975
47. Spoerke, E. D., McKenzie, B. B., Bell, N. S., Edney, C., Wheeler, J. S., & Ingersoll, D. (n.d.). Characterization of phase chemistry in sol-gel NASICON (Rep.). Retrieved <https://www.sandia.gov/essssl/EESAT/2013_papers/Characterization_of_Phase_Chemistry_in_Sol-Gel_NaSICON.pdf>
48. Ahmad, A., Wheat, T., Kuriakose, A., Canaday, J., & Mcdonald, A. (1987). Dependence of the properties of Nasicons on their composition and processing. Solid State Ionics, 24(1), 89-97. doi:10.1016/0167-2738(87)90070-1
49. Fabrication and characterization of nasicon ceramic electrolytes. (1980). Journal of Power Sources, 5(4), 413-415. doi:10.1016/0378-7753(80)80083-8
50. Mcentire, B., Bartlett, R., Miller, G., & Gordon, R. (1982). Effect of decomposition on the densification and properties of NASICON ceramic electrolytes. doi:10.2172/5234213
51. Vonalpen, U., Bell, M., & Hofer, H. (1981). Compositional dependence of the electrochemical and structural parameters in the Nasicon system (Na1 xSixZr2P3−xO12). Solid State Ionics, 3-4, 215-218. doi:10.1016/0167-2738(81)90085-0

52. Traversa, E., Montanaro, L., Aono, H., & Sadaoka, Y. (2000). Synthesis of NASICON with New Compositions for Electrochemical Carbon Dioxide Sensors. Journal of Electroceramics, 5(3), 261-272. doi:10.1023/a:1026543915883
53. Kreuer, K., & Warhus, U. (1986). NASICON solid electrolytes: Part IV Chemical durability. Materials Research Bulletin, 21(3), 357-363. doi:10.1016/0025-5408(86)90193-5
54. Schmid, H., Dejonghe, L., & Cameron, C. (1982). Chemical stability of Nasicon. Solid State Ionics, 6(1), 57-63. doi:10.1016/0167-2738(82)90096-0
55. Fuentes, R. (2001). Reaction of NASICON with water. Solid State Ionics, 139(3-4), 309-314. doi:10.1016/s0167-2738(01)00683-x
56. Agrawal, D. K., & Adair, J. H. (1990). ChemInform Abstract: Low-Temperature Sol-Gel Synthesis of NaZr2P3O12. ChemInform, 21(42). doi:10.1002/chin.199042035
57. Mauvy, F. (1999). Reactivity of NASICON with water and interpretation of the detection limit of a NASICON based Na ion selective electrode. Talanta, 48(2), 293-303. doi:10.1016/s0039-9140(98)00234-3
58. Spoerke, E. D., Bell, N., Delnick, F., Edney, C., & McKenzie, B. (n.d.). Synthesis and Stability of NASICON for Sodium Based Batteries. ESS 2012 Peer Review
59. Jung, J., Kim, D., Kim, H., Jo, Y. N., Park, J. S., & Kim, Y. (2016). Progressive Assessment on the Decomposition Reaction of Na Superionic Conducting Ceramics. ACS Applied Materials & Interfaces, 9(1), 304-310. doi:10.1021/acsami.6b09316
60. Lunghammer, S., Ma, Q., Rettenwander, D., Hanzu, I., Tietz, F., & Wilkening, H. (2018). Bulk and grain-boundary ionic conductivity in sodium zirconophosphosilicate Na 3 Zr 2 (SiO 4) 2 PO 4 (NASICON). Chemical Physics Letters, 701, 147-150. doi:10.1016/j.cplett.2018.04.037
61. Nasiri-Tabrizi, B. (2014). Thermal treatment effect on structural features of mechano-synthesized fluorapatite-titania nanocomposite: A comparative study. Journal of Advanced Ceramics, 3(1), 31-42. doi:10.1007/s40145-014-0090-4
62. Komorowski, P., Argyropoulos, S., Hancock, R., Gulens, J., Taylor, P., Canaday, J., . . . Ahmad, A. (1991). Characterization of protonically exchanged NASICON. Solid State Ionics, 48(3-4), 295-301. doi:10.1016/0167-2738(91)90046-e
63. Gulens, J. (1989). Influence of water on the electrochemical response of a bonded nasicon protonic conductor. Solid State Ionics, 35(1-2), 45-49. doi:10.1016/0167-2738(89)90010-6
64. Winkler, B., Avalos-Borja, M., Milman, V., Perlov, A., Pickard, C. J., & Yates, J. R. (2013). Oxygen K-edge electron energy loss spectra of hydrous and anhydrous compounds. Journal of Physics: Condensed Matter, 25(48), 485401. doi:10.1088/0953-8984/25/48/485401

65. Sundell, P. G., Björketun, M. E., & Wahnström, G. (2006). Thermodynamics of doping and vacancy formation in BaZrO3 perovskite oxide from density functional calculations. Physical Review B, 73(10). doi:10.1103/physrevb.73.104112
66. Bollinger, M. V., Jacobsen, K. W., & Nørskov, J. K. (2003). Atomic and electronic structure of MoS2 nanoparticles [Phys. Rev. B67, 085410 (2003)]. Physical Review B, 67(12). doi:10.1103/physrevb.67.129906
67. Didisheim, J., Prince, E., & Wuensch, B. (1986). Neutron Rietveld analysis of structural changes in NASICON solid solutions Na1 xZr2SixP3−xO12 at elevated temperatures: X=1.6 and 2.0 at 320°C. Solid State Ionics, 18-19, 944-958. doi:10.1016/0167-2738(86)90291-2
68. Smallmas, R. E., & Ngan, A. H. (2007). Physical Metallurgy and Advanced Materials (7th ed.).
69. Shafi, P. M., & Bose, A. C. (2015). Impact of crystalline defects and size on X-ray line broadening: A phenomenological approach for tetragonal SnO2 nanocrystals. *AIP Advances, 5*(5), 057137. doi:10.1063/1.4921452

6. Acknowledgment

Before I start to the main points, I would like to express my appreciation to the god that allows me to meet everyone during my master study. I would also want to say thank you for the support from my family for always supporting my back no matter the problem that I'm facing in. Without their help, I don't think that I am able to finish my study in UNIST.

The master study that I did in seawater battery was quite memorable, and I feel quite lucky to be in this lab. I would like to express my special thanks to my advisor, Prof. Youngsik Kim, for this opportunity. He always never gives up on me and give me guidance during my research study. I also want to say thank you to Prof. Hyun-Wook Lee for always supporting me whenever I have a problem. If I become a professor in the future, I would remember Prof. Youngsik Kim and Prof. Hyun-Wook Lee as my role model. I also would also like to express my appreciation to Prof. Sangkyu Kwak to support me for the project and Prof. Yoonseok Choi for helping me in my thesis. I hope you the best in your careers and life.

For the lab member and solid electrolyte team, I would like to give you my special thanks. There are a lot of things that I want to express, but 1 page is not enough to show my gratefulness to everyone. You always treat me as a family and I am very happy to be one of the lab member as well as solid electrolyte team. For Wooseok and Mr. Jinho Pyo (공장장님), I would like to say thanks for your guidance during my research. Without you, I don't think I am able to graduate from UNIST. I wish you all the best in your career inside and outside the lab. One more time I would like to express that I am happy and lucky to meet you in the lab. It was fun, and I appreciate for you accompany.

For my friend (Indonesian and International friend) and my sweetheart, Lulu, thank you for always supporting me whenever I am down. With you in my back, I can keep moving forward and tackle all the problem. For my friend (and lab member and research team), no matter how far you are, I will always remember you like the first time we met. So, please don't hesitate to contact me through email (rahmanmfahmi@gmail.com) whenever you need it.

In conclusion, I would like to express my thanks to everyone. I wish that this is not the last time we meet each other. This might be the end of my chapter in Korea and I hope that we can meet again in the future. And if you ever come to Indonesia, please feel free to contact me. I would gladly welcome you to my country. Lastly, I would like to say that it was fun knowing you and see you in the future.